Biochemical and Biophysical Research Communications 391 (2010) 1222–1227

Contents lists available at ScienceDirect

Biochemical and Biophysical Research Communications

journal homepage: www.elsevier.com/locate/ybbrc

The liver-enriched transcription factor CREBH is nutritionally regulated and activated by fatty acids and PPARα

Hirosuke Danno, Kiyo-aki Ishii [1], Yoshimi Nakagawa [1], Motoki Mikami, Takashi Yamamoto, Sachiko Yabe, Mika Furusawa, Shin Kumadaki, Kazuhisa Watanabe, Hidehisa Shimizu, Takashi Matsuzaka, Kazuto Kobayashi, Akimitsu Takahashi, Shigeru Yatoh, Hiroaki Suzuki, Nobuhiro Yamada, Hitoshi Shimano *

Department of Internal Medicine (Endocrinology and Metabolism), Graduate School of Comprehensive Human Sciences, University of Tsukuba, 1-1-1 Tennodai, Tsukuba Ibaraki 305-8575, Japan

ARTICLE INFO

Article history:
Received 26 November 2009
Available online 16 December 2009

Keywords:
Fasting
Refeeding
Starvation
ER stress
PPRE

ABSTRACT

To elucidate the physiological role of CREBH, the hepatic mRNA and protein levels of CREBH were estimated in various feeding states of wild and obesity mice. In the fast state, the expression of CREBH mRNA and nuclear protein were high and profoundly suppressed by refeeding in the wild-type mice. In ob/ob mice, the refeeding suppression was impaired. The diet studies suggested that CREBH expression was activated by fatty acids. CREBH mRNA levels in the mouse primary hepatocytes were elevated by addition of the palmitate, oleate and eicosapenonate. It was also induced by PPARα agonist and repressed by PPARα antagonist. Luciferase reporter gene assays indicated that the CREBH promoter activity was induced by fatty acids and co-expression of PPARα. Deletion studies identified the PPRE for PPARα activation. Electrophoretic mobility shift assay and chromatin immunoprecipitation (ChIP) assay confirmed that PPARα directly binds to the PPRE. Activation of CREBH at fasting through fatty acids and PPARα suggest that CREBH is involved in nutritional regulation.

Introduction

The liver-enriched bZip transcription factor, CREBH belongs to the CREB family. It activates transcription through binding to cAMP responsive element (CRE) and box B element [1]. It is a membrane-bound protein located on the endoplasmic reticulum via Leucine-zipper domain. Upon ER stress, it shifts on a Golgi, N-terminal fragment is processed by Site 1 protease and Site 2 proteases known to also work on SREBPs, traffics to the nucleus to activate transcription of acute inflammatory genes such as serum amyloid P (SAP), C-reactive protein (CRP) via CRE [2]. It also trans-activates the gluconeogenesis enzyme phosphoenolpyruvate carboxykinase (PEPCK) through direct binding to CRE. This activation can be further stimulated by cAMP and protein kinase A [3]. Although these previous studies suggest involvement of this membrane-bound transcription factor in nutrition, its precise function and nutritional regulation are not fully understood.

Non-esterified fatty acids or their CoA derivatives are the main signals involved in the transcriptional effect of long-chain fatty acids. The effects of fatty acids are mediated either directly owing to their specific binding to nuclear receptors (PPAR and HNF4α) leading to changes in the trans-activating activity of these transcription factors. During fasting, fatty acids are released from adipose tissue and travel to the liver, where they bind and activate PPARα. Activation of PPARα results in stimulation of a number of pathways, including fatty acid oxidation, ketogenesis and suppression of amino acid catabolism. In this way, endogenous ligand-activation of PPARα occurs primarily during fasting as large amounts of free fatty acids enter the blood plasma [4,5]. Dietary intake of specific fatty acids can lead to potent activation of PPARα [6]. In addition to a host of endogenous ligands, PPARα is the molecular target for fibrates, which are synthetic PPARα agonists that include bezafibrate and fenofibrate [7]. PPARα regulates gene transcription by heterodimerizing with RXR (retinoid X receptor). PPAR/RXR heterodimers bind to a specific DNA sequence, peroxisome proliferator responsive element (PPRE). The consensus sequence consists of a direct repeat element (AGGTCA) with an interspacing of one or two base pair (DR1 or DR2) with a 5′-A/T rich flanking sequence which is essential for the polarity of DNA binding of the heterodimer PPAR/RXR [8].

In the current study, nutritional regulation of hepatic CREBH expression was examined in various feeding states and diabetic mice and its promoter was investigated as a new target of PPARα.

* Corresponding author. Fax: +81 29 853 3174.
E-mail address: hshimano@md.tsukuba.ac.jp (H. Shimano).
[1] These authors equally contributed to this work.

0006-291X/$ - see front matter © 2009 Elsevier Inc. All rights reserved.
doi:10.1016/j.bbrc.2009.12.046

Materials and methods

Animal experiments. For all experiments, 8-week-old male C57BL/6 mice from CLEA Japan were used. Mice were maintained on a standard chow diet. For diet-induced obesity (DIO), C57BL/6 mice were fed high-fat/high-sucrose (HF/HS) diet for 12 weeks. For fasting/refeeding protocol, mice were fasted for 24 h and then fed various diets for 12 h. Feed ingredient contents are as follows. Standard chow diet consists of carbohydrate 60%, protein 23.6%, fat 5.3%. High-sucrose diet consists of carbohydrate 70%, protein 20%, fat-free. High-fat diet consists of carbohydrate 27.5%, protein 25.6%, fat 35%. High-fat/high-sucrose diet consists of carbohydrates 34.8%, protein 25%, fat 30% (ORIENTAL YEAST Co., Ltd.).

Total RNA preparation, northern blotting and quantitative real-time PCR analysis. Total RNA from cell and tissues were prepared using Trizol reagent (Invitrogen) unless otherwise indicated. Northern blot analysis was performed as previously described [9]. cDNA probe for CREBH was prepared from reverse transcriptase for PCR using mouse liver mRNA (422–1861 bp, Genbank Accession No. NM_145365). Quantitative real-time PCR analysis was performed as described previously [10].

The primer sets were as follows; CREBH forward, 5′-CCAGAGC CCTTTACCCATACAT-3′, CREBH reverse, 5′-ATGGTTGGAGGTTAGG GTTCAG-3′, CPT1a forward, 5′-CCTGGGCATGATTGCAAAG-3′, CPT1a reverse, 5′-GGACGCCACTCACGATGTT-3′, MCAD forward, 5′-TGCTT TTGATAGAACCAGACCTACAGT-3′, MCAD reverse, 5′-CTTGGTGCTCC ACTAGCAGCTT-3′, ACO forward, 5′-CGATCCAGACTTCCAACATG AG-3′, ACO reverse, 5′-CCATGGTGGCACTCTTCTTAACA-3′.

Immunoblotting. Immunoblot analysis of nuclear extracts from livers of fasted or refed mice was as previously described [9]. For each group, livers from three mice were pooled, and aliquots (10 μg of protein) of nuclear extracts were subjected to immunoblot analysis with rabbit anti-mouse CREBH as primary antibody and anti-rabbit IgG, HRP-linked antibody (Cell signalling technology) as the secondary antibody. Anti-mouse CREBH rabbit polyclonal antibody was prepared using GST-mouse CREBH (amino acid 1–85).

Isolation and culture of hepatocytes and fatty acid administration. Primary hepatocytes were isolated from male mice and cultured in Dulbecco's modified Eagle's medium (DMEM) high glucose supplemented with 10% fetal calf serum (FCS), 100 nM insulin, 10 nM dexamethasone, 1% penicillin/streptomycin prior to transfer to 60-mm collagen dishes at a final density 3.5×10^4 cells cm^{-2}. After incubation for 6 h for attachment, the medium was replaced with FCS free DMEM low glucose with 0.5% bovine serum albumin (BSA), 10 nM dexamethasone, 10 mM lactate for 16 h, followed by fatty acid administration for 8 h.

To examine effects of PPARα agonist and antagonist on the CREBH mRNA level in mouse primary hepatocytes, cells were supplemented with media alone or media containing PPARα antagonist (MK886) for 24 h, then after administered PPARα agonist (fenofibrate) for 8 h.

Plasmids. The expression vector for mouse PPARα was generated by inserting PCR-amplified full-length fragment into pcDNA3.1(+) (Invitrogen) containing a CMV promoter. The mouse CREBH promoter (base pairs −2000 to −1, relative to the transcriptional start site) was amplified by PCR using mouse BAC (Bacterial Artificial Chromosome). The primers were tailed with KpnI site (5′primers) or BglII site (3′primer). The PCR products were digested with KpnI and BglII and subcloned into pGL3-basic luciferase vector (Promega). Other constructs were produced by PCR using this construct as DNA template and subcloned the PCR products into the pGL3-basic luciferase vector.

Identification of the transcription start point. The transcription start point was determined by a PCR-based restricted fragment length analysis; DNA fragments amplified from mouse liver cDNA by PCR using four primer sets designed as follows; (exon 1 forward, 5′-GCTGTGGTGTGTCTCTGTCC-3′, exon1 reverse, 5′-ACAGGAAGAG CAGCTGCC-3′) (exon 1 forward, 5′-GCTGTGGTGTGTCTCTGTCC-3′, exon 2 reverse, 5′-ACTGTTTCTGTCTAGCGTCACC-3′) (exon 2 forward, 5′-AGCTGGCAACCTACCCAAG-3′, exon 3 reverse, 5′-CTTTCCA GCCGCTATGTCC-3′) (exon forward, 5′-CATCTTTGGGAGGTGGAG AC-3′, exon 4 reverse, 5′-CTCCACGTTTCTCAGGATGC-3′).

Transfection and luciferase assays. HepG2 cells were transfected with 200 ng each of indicated luciferase reporter and expression plasmids (CMV-PPARα or basic plasmid CMV7 as negative control) and a pRL-SV40 plasmid as a reference (Promega) using FuGENE6 (Roche). After a 24 h incubation at 37 °C, we measured the amount of firefly luciferase activity and normalized it to the amount of renilla luciferase activity.

Electrophoretic mobility shift assay (EMSA). Human PPARα and RXRα proteins were generated from the full-length human PPARα and RXRα expression vectors (pCI-PPARα and CMX-RXRα), respectively, using the TNT T7 Quick-coupled transcription/translation system (Promega). The probes for PPARα binding site were as follows: rat PEPCK promoter (−908 to −873 bp), gtcactcccacGGCC AAAGGTCAtgagaagggaatt; mouse CREBH promoter (−188 to −156 bp), gagctgtaagtAGGGGAGAGGTCAcacagacccg. Double-stranded oligonucleotides used in EMSA were labelled with [α-^{32}P]dCTP

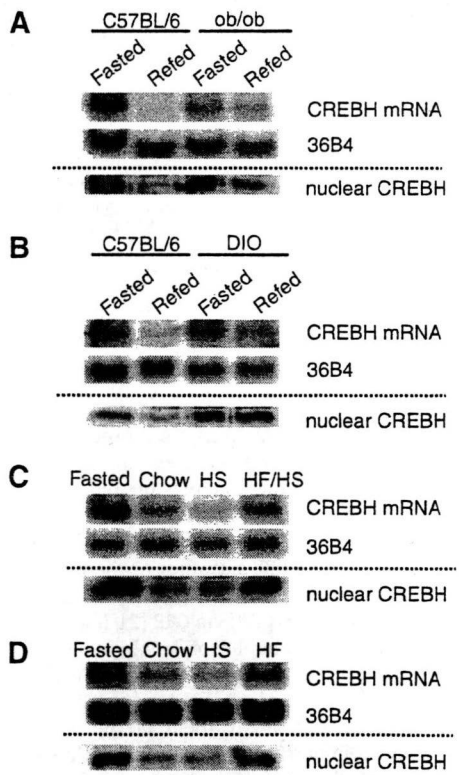

Fig. 1. Hepatic mRNA and protein levels of CREBH in various feeding states and obesity mice. (A) The expression of CREBH in the livers of wild-type and ob/ob mice. Mice were fasted for 24 h or fasted for 24 h/refed for 12 h. Both mice were fed HS diet during the refeeding period. (B) The expression of CREBH in the livers of wild-type and DIO (HF/HS diet for 12 weeks) mice. Mice were fasted for 24 h or fasted for 24 h/refed for 12 h. Wild-type mice were fed HS diet, DIO mice were fed HF/HS diet during the refeeding period. (C) The expression of CREBH in the livers of wild-type fed various diets. Mice were fasted for 24 h or fasted for 24 h/refed for 12 h. Mice were fed standard chow, HS and HF/HS diet during the refeeding period. (D) The expression of CREBH in the livers of wild-type fed various diets. Mice were fasted for 24 h or fasted for 24 h/refed for 12 h. Mice were fed standard chow, HS and HF diet during the refeeding period. Upper panel shows Northern blot, lower panel shows Western blot in nuclear extracts (nuclear CREBH). ($n = 3$ per group).

using Klenow fragment, followed by purification on Sephadex G25 columns (GE Healthcare). The labelled probes were incubated with 4 μl of in vitro-translated protein in 15 μl mixtures containing 10 mM Hepes (pH 7.8), 50 mM KCl, 1 mM EDTA, 5 mM $MgCl_2$, 10% glycerol, 1 mM dithiothreitol and 26.6 mg/ml poly(dI-dC) for 30 min at room temperature. The DNA–protein complexes were resolved by 4.5% PAGE at 90 V for 1.5 h at room temperature. Gels were dried and analyzed using a GEL DRYER MODEL583 (BIO-RAD Laboratories).

Chromatin immunoprecipitation (ChIP) assays. ChIP assays were performed using a Simple ChIP Enzymatic Chromatin IP Kit (Cell signalling technology). Immunoprecipitation was performed using an antibody directed against PPARα (H-98; Santa Cruz Biotechnology) or with rabbit IgG (Santa Cruz Biotechnology) as a negative control. After immunoprecipitation, associated DNA was amplified with a primer pair containing PPRE, −337 to −137 bp (forward 5′-ACAGGGTTAGCGGTTGTCAC-3′ and reverse 5′-AGAGCAAAGTCTG GGGTGTC-3′).

Statistical analysis. Data are expressed as means ± SEM. Statistical significance was tested with an unpaired two-tailed Student's *t*-test. The difference were considered to be significant at $P < 0.05$.

Results and discussion

To see the nutritional regulation of CREBH gene expression, CREBH mRNA level was compared in livers of C57BL/6 mice at fasting and refeeding. Hepatic CREBH mRNA expression was robust in a fasted state, and profoundly suppressed after refeeding with a sucrose diet (Fig. 1A). Immunoblot analysis demonstrated that hepatic nuclear protein level was similarly upregulated at fasting and downregulated at refeeding indicating that the change in mRNA could be associated with regulation of its activity as a transcription factor. Intriguingly, the refeeding suppression of CREBH mRNA and nuclear protein was diminished in genetically leptin-deficient obesity model, ob/ob mice, supporting the nutritional regulation of CREBH. When mice were put on high-fat and high-sucrose diet to cause diet-induced obesity (12 weeks), the fasting/refeeding regulation was impaired (Fig. 1B). CREBH expression and activity were sustained at fasting, but exhibited no remarkable change after refeeding. Effects of diet contents on suppression of CREBH expression were investigated among control, high-sucrose, high-fat, and high-fat/high-sucrose diets. As shown in Fig. 1C and D, while feeding suppression was most marked on a high carbohydrate diet, high-fat diet was the weakest inhibitor. The nuclear protein followed in a similar pattern. Intriguingly, these nutritional changes in CREBH expression level were strongly associated with plasma levels of free fatty acids. Plasma non-esterified fatty acid concentration of normal C57BL/6 mice in fated and refed states were as follows: 0.93 ± 0.07 mEq/l in the fasted state, 0.93 ± 0.21 mEq/l fed on the high-fat diet, 0.38 ± 0.07 mEq/l on the high-fat/high-sucrose diet, 0.36 ± 0.05 mEq/l on the chow diet, and 0.18 ± 0.00 mEq/l on the high-sucrose diet ($n = 3$ per group).

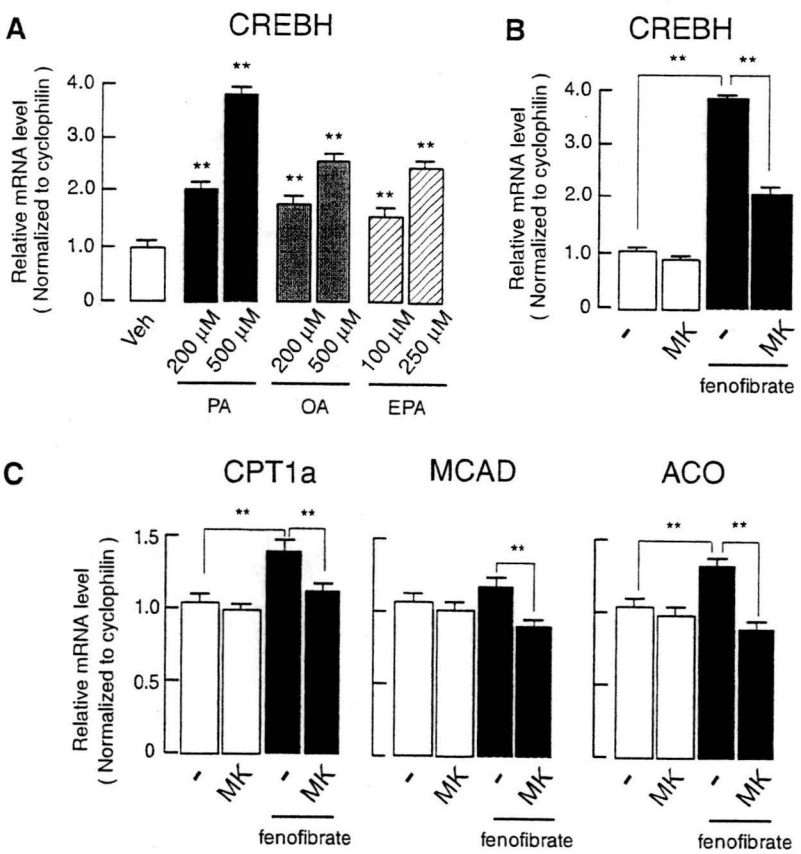

Fig. 2. Effects of free fatty acids and PPARα agonist and antagonist on CREBH mRNA in HepG2 cells. (A) Effect of fatty acids on the expression of CREBH in mouse primary hepatocytes. Cells were supplemented with media alone (fatty acid-free) or media containing 200/500 μM palmitic acid (PA), 200/500 μM oleic acid (OA), 100/250 μM eicosapentanoic acid (EPA) for 8 h before RNA extraction. The CREBH mRNA levels were estimated by RT-PCR analysis, normalized to cyclophilin. (B, C) Effect of PPARα agonist and antagonist on gene expression in mouse primary hepatocytes. The expression of CREBH (B) and PPARα-regulated genes (C) were estimated by RT-PCR analysis, normalized to cyclophilin. CPT1a (carnitine palmitoyltransferase 1a), MCAD (medium chain acyl-CoA dehydrogenase), ACO (acyl-CoA oxidase). Results are represented as means ± SEM ($n = 3$). **$P < 0.01$, compared with vehicle treated cells.

To test possibility of regulation by fatty acids, CREBH expression was investigated in primary hepatocytes incubated with various fatty acids. Palmitate (PA), oleate (OA), and eicosapentaenoate (EPA) dose-dependently at regular concentrations increased CREBH expression, but there were no marked differences among these fatty acids (Fig. 2A). Based upon these responses on fasting induction and fatty acid enhancement, involvement of PPARα in CREBH regulation was speculated and tested. Treatment of fenofibrate, a PPARα agonist increased CREBH expression and this induction was cancelled by further addition of a PPARα inhibitor, MK886 (Fig. 2B). Similar changes were observed in expression of PPARα target genes such as CPT1a, MCAD, and ACO, confirming activation and cancellation of PPARα by these agents (Fig. 2C).

Next, mouse CREBH promoter was investigated. The gene structure of mouse CREBH was shown in Fig. 3A based upon reported sequence information (Ensembl Genome Browser). While exon 3 containing ATG translation start site was detected by RT-PCR of mouse liver RNAs, untranslated exons 1 and 2 were not detectable in our experimental settings. Exon 3 has been reported as another transcription start site by the Ensembl Genome Browser. Our data indicated that the transcription primarily starts from exon 3 in the liver. The upstream 2 kb region contained a few potential PPREs and was cloned into a pGL3 luciferase reporter (Fig. 3A). Using this construct, CREBH promoter activity was tested in the light of PPARα activation in HepG2 cells. Co-expression of PPARα markedly activated the promoter activity (Fig. 3B). The promoter activity was increased by incubation with PA, OA, and EPA, consistent with increases in CREBH mRNA (Fig. 3C). To identify the functional PPRE sites (Fig. 3A), various deletion constructs as indicated in Fig. 4A were prepared and tested in the basal and PPARα-induced activities. The region responsible for PPARα activation was located between −189 and −164 bp, indicating that the PPRE sequence at −178 to −166 bp was crucial for PPARα activation (Fig. 4B). EMSA using this sequence demonstrated that PPARα/RXRα complex binds strongly to this lesion (Fig. 4C). ChIP assay of genomic DNA from mouse liver confirmed direct binding of PPARα to this PPRE in vivo and the signal detected at fasting was suppressed by refeeding, consistent with dietary regulation of CREBH expression (Fig. 4C).

CREBH has been reported to be activated by ER stress through proteolytic cleavage and involved in ER stress response genes [2]. Our data demonstrated that CREBH is nutritionally regulated at the transcription level and activated by fasting and fatty acids. Although both fasting and fatty acids could be a part of ER stress, current data indicated that CREBH is regulated by PPARα, which could at least partially explain for activation by fasting and fatty acids. It was also reported that CREBH was transcriptionally activated by HNF4α [11]. Our data also indicated that HNFα transactivation could be both direct and indirect through PPARα activation because PPARα is an HNF4α target [12]. Nutritional regulation of

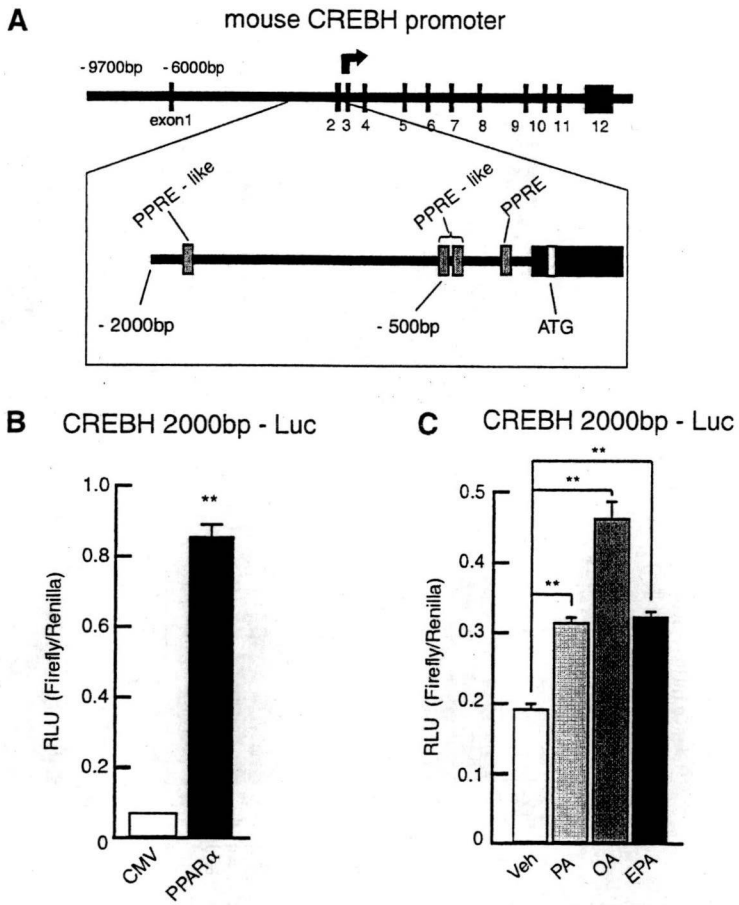

Fig. 3. Activation of the mouse CREBH promoter by PPARα and free fatty acids in luciferase reporter gene assay in HepG2 cells. (A) The schematic presentation of mouse CREBH promoter. (B) Effects of PPARα on mouse CREBH promoter activity in HepG2 cells as estimated by luciferase reporter assay. (C) Effects of free fatty acids on mouse CREBH promoter activity in HepG2 cells, as estimated by luciferase reporter assay. Cells were supplemented with media alone (fatty acid-free) or media containing 500 μM palmitic acid (PA), 500 μM oleic acid (OA), 250 μM eicosapentanoic acid (EPA) for 8 h. Results are represented as means ± SEM ($n = 3$). $^{**}P < 0.01$, compared with vehicle treated cells.

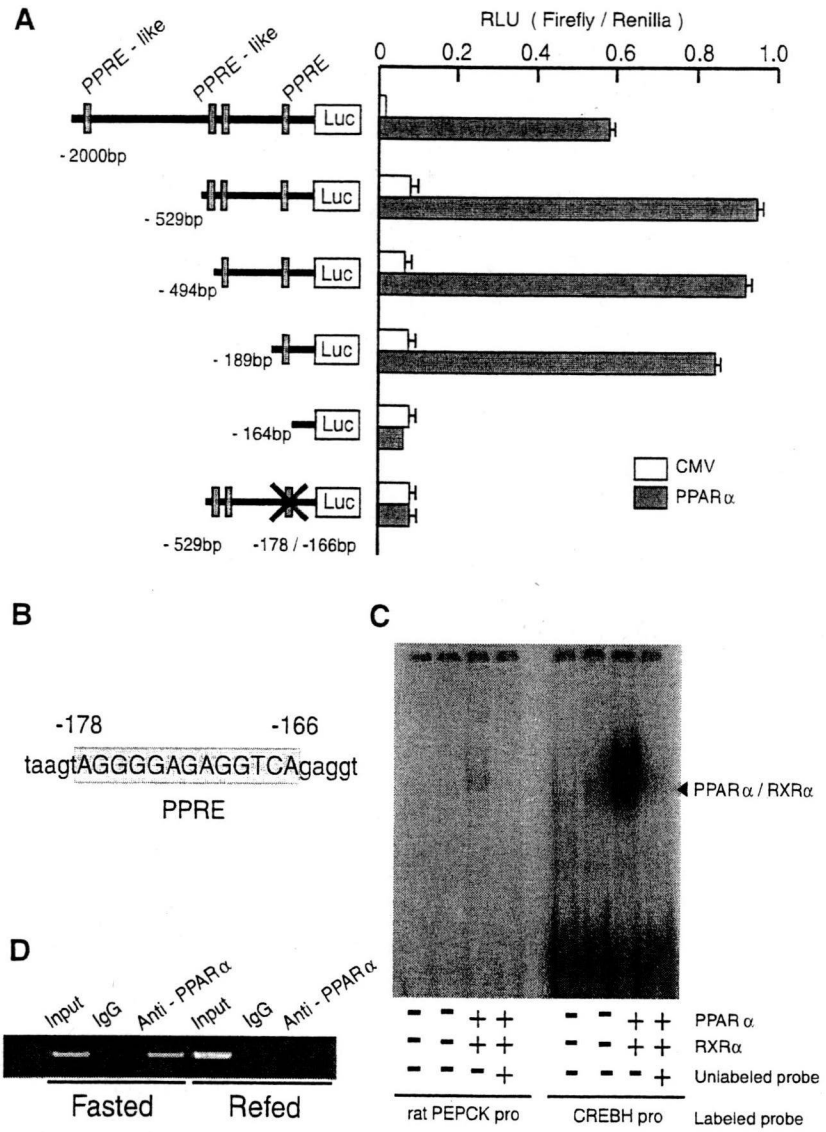

Fig. 4. Mouse CREBH promoter is a direct target of PPARα. (A) Luciferase assays of the luciferase reporter gene mCREBH 2000 bp-Luc and its various deletion constructs in the presence or absence of the PPARα expression plasmid in HepG2 cells (B) PPRE of the mouse CREBH promoter (C) EMSA for PPARα/RXRα binding to PPRE of CREBH promoter. Aliquots of 2 μl of in vitro-translated PPARα and/or 2 μl of RXRα were incubated with ^{32}P-labelled rat PEPCK promoter probe (as positive control) and CREBH promoter probe in the presence or absence unlabeled probe. (D) ChIP assay for PPARα binding to PPRE of the CREBH promoter using liver samples from mice fasted or refed. The extracted genomic DNA was subjected to immunoprecipitation, performed using an antibody against PPARα or with IgG as a negative control. For comparison, amplification derived from unprecipitated chromatin is also shown (input).

CREBH suggested that CREBH might possess its new function in energy metabolism at starvation, which is currently under investigation.

Acknowledgments

This work was supported by Grants-in-Aid from the Ministry of Science, Education, Culture, and Technology of Japan, Japan Diabetes Foundation, Astellas Foundation for Research on Metabolic Disorders, Kanae Foundation for The Promotion of Medical Science, The Uehara Memorial Foundation, and Suzuken Memorial Foundation.

References

[1] Y. Omori, J. Imai, M. Watanabe, T. Komatsu, Y. Suzuki, K. Kataoka, S. Watanabe, A. Tanigami, S. Sugano, CREB-H: a novel mammalian transcription factor belonging to the CREB/ATF family and functioning via the box-B element with a liver-specific expression, Nucleic Acids Res. 29 (2001) 2154–2162.
[2] K. Zhang, X. Shen, J. Wu, K. Sakaki, T. Saunders, D.T. Rutkowski, S.H. Back, R.J. Kaufman, Endoplasmic reticulum stress activates cleavage of CREBH to induce a systemic inflammatory response, Cell 124 (2006) 587–599.
[3] K.T. Chin, H.J. Zhou, C.M. Wong, J.M. Lee, C.P. Chan, B.Q. Qiang, J.G. Yuan, I.O. Ng, D.Y. Jin, The liver-enriched transcription factor CREB-H is a growth suppressor protein under expressed in hepatocellular carcinoma, Nucleic Acids Res. 33 (2005) 1859–1873.
[4] S. Kersten, J. Seydoux, J.M. Peters, F.J. Gonzalez, B. Desvergne, W. Wahli, Peroxisome proliferator-activated receptor alpha mediates the adaptive response to fasting, J. Clin. Invest. 103 (1999) 1489–1498.
[5] T.C. Leone, C.J. Weinheimer, D.P. Kelly, A critical role for the peroxisome proliferator-activated receptor alpha (PPARalpha) in the cellular fasting response: the PPARalpha-null mouse as a model of fatty acid oxidation disorders, Proc. Natl. Acad. Sci. USA 96 (1999) 7473–7478.
[6] B. Ren, A. Thelen, D.B. Jump, Evidence against the peroxisome proliferator-activated receptor alpha as the mediator of polyunsaturated fatty acid regulation of s14 gene transcription, J. Biol. Chem. 271 (1996) 17167–17173.
[7] J.C. Fruchart, P. Duriez, B. Staels, Molecular mechanism of action of the fibrates, J. Soc. Biol. 193 (1999) 67–75.

[8] B. Desvergne, W. Wahli, Peroxisome proliferator-activated receptors: nuclear control of metabolism, Endocr. Rev. 20 (1999) 649–688.
[9] H. Shimano, N. Yahagi, M. Amemiya-Kudo, A.H. Hasty, J. Osuga, Y. Tamura, F. Shionoiri, Y. Iizuka, K. Ohashi, K. Harada, T. Gotoda, S. Ishibashi, N. Yamada, Sterol regulatory element-binding protein-1 as a key transcription factor for nutritional induction of lipogenic enzyme genes, J. Biol. Chem. 274 (1999) 35832–35839.
[10] T. Kato, H. Shimano, T. Yamamoto, T. Yokoo, Y. Endo, M. Ishikawa, T. Matsuzaka, Y. Nakagawa, S. Kumadaki, N. Yahagi, A. Takahashi, H. Sone, H. Suzuki, H. Toyoshima, A.H. Hasty, S. Takahashi, H. Gomi, T. Izumi, N. Yamada, Granuphilin is activated by SREBP-1c and involved in impaired insulin secretion in diabetic mice, Cell. Metab. 4 (2006) 143–154.
[11] J. Luebke-Wheeler, K. Zhang, M. Battle, K. Si-Tayeb, W. Garrison, S. Chhinder, J. Li, R.J. Kaufman, S.A. Duncan, Hepatocyte nuclear factor 4alpha is implicated in endoplasmic reticulum stress-induced acute phase response by regulating expression of cyclic adenosine monophosphate responsive element binding protein H, Hepatology 48 (2008) 1242–1250.
[12] I. Pineda Torra, Y. Jamshidi, D.M. Flavell, J.C. Fruchart, B. Staels, Characterization of the human PPARalpha promoter: identification of a functional nuclear receptor response element, Mol. Endocrinol. 16 (2002) 1013–1028.

Circulation Research

JOURNAL OF THE AMERICAN HEART ASSOCIATION

American Heart Association®

Learn and Live℠

Activating Transcription Factor 3 Constitutes a Negative Feedback Mechanism That Attenuates Saturated Fatty Acid/Toll-Like Receptor 4 Signaling and Macrophage Activation in Obese Adipose Tissue

Takayoshi Suganami, Xunmei Yuan, Yuri Shimoda, Kozue Uchio-Yamada, Nobutaka Nakagawa, Ibuki Shirakawa, Takako Usami, Takamitsu Tsukahara, Keizo Nakayama, Yoshihiro Miyamoto, Kazuki Yasuda, Junichiro Matsuda, Yasutomi Kamei, Shigetaka Kitajima and Yoshihiro Ogawa

Circ. Res. 2009;105;25-32; originally published online May 28, 2009;
DOI: 10.1161/CIRCRESAHA.109.196261
Circulation Research is published by the American Heart Association. 7272 Greenville Avenue, Dallas, TX 72514
 Print ISSN: 0009-7330. Online ISSN: 1524-4571

Activating Transcription Factor 3 Constitutes a Negative Feedback Mechanism That Attenuates Saturated Fatty Acid/Toll-Like Receptor 4 Signaling and Macrophage Activation in Obese Adipose Tissue

Takayoshi Suganami, Xunmei Yuan, Yuri Shimoda, Kozue Uchio-Yamada, Nobutaka Nakagawa, Ibuki Shirakawa, Takako Usami, Takamitsu Tsukahara, Keizo Nakayama, Yoshihiro Miyamoto, Kazuki Yasuda, Junichiro Matsuda, Yasutomi Kamei, Shigetaka Kitajima, Yoshihiro Ogawa

Abstract—Obese adipose tissue is markedly infiltrated by macrophages, suggesting that they may participate in the inflammatory pathways that are activated in obese adipose tissue. Evidence has suggested that saturated fatty acids released via adipocyte lipolysis serve as a naturally occurring ligand that stimulates Toll-like receptor (TLR)4 signaling, thereby inducing the inflammatory responses in macrophages in obese adipose tissue. Through a combination of cDNA microarray analyses of saturated fatty acid–stimulated macrophages in vitro and obese adipose tissue in vivo, here we identified activating transcription factor (ATF)3, a member of the ATF/cAMP response element-binding protein family of basic leucine zipper-type transcription factors, as a target gene of saturated fatty acids/TLR4 signaling in macrophages in obese adipose tissue. Importantly, ATF3, when induced by saturated fatty acids, can transcriptionally repress tumor necrosis factor-α production in macrophages in vitro. Chromatin immunoprecipitation assay revealed that ATF3 is recruited to the region containing the activator protein-1 site of the endogenous tumor necrosis factor-α promoter. Furthermore, transgenic overexpression of ATF3 specifically in macrophages results in the marked attenuation of proinflammatory M1 macrophage activation in the adipose tissue from genetically obese KKA^y mice fed high-fat diet. This study provides evidence that ATF3, which is induced in obese adipose tissue, acts as a transcriptional repressor of saturated fatty acids/TLR4 signaling, thereby revealing the negative feedback mechanism that attenuates obesity-induced macrophage activation. Our data also suggest that activation of ATF3 in macrophages offers a novel therapeutic strategy to prevent or treat obesity-induced adipose tissue inflammation. (*Circ Res.* 2009;105:25-32.)

Key Words: adipocytes ■ ATF3 ■ fatty acids ■ inflammation ■ macrophages ■ TLR4

Known as the metabolic syndrome, the cluster of well-established risk factors for cardiovascular disease (visceral fat obesity, impaired glucose metabolism, atherogenic dyslipidemia, and blood pressure elevation), is an increasing health problem worldwide.[1–3] The pathophysiology underlying the metabolic syndrome is not fully understood and visceral fat obesity appears to be an important component.[4] There is considerable evidence that obesity is a state of chronic low-grade inflammation, which may play a critical role in the pathophysiology of the metabolic syndrome.[1–3]

Obese adipose tissue is markedly infiltrated by macrophages, suggesting that they may participate in the inflammatory pathways that are activated in obese adipose tissue.[5] Using an in vitro coculture system composed of adipocytes and macrophages, we have provided evidence that a paracrine loop involving saturated fatty acids and tumor necrosis factor (TNF)α derived from adipocytes and macrophages, respectively, establishes a vicious cycle that augment the inflammatory change in obese adipose tissue.[6] Recent studies have also pointed to the heterogeneity of macrophages infiltrated into obese adipose tissue, ie, they follow 2 different polarization states: M1, or "classically activated" (proinflammatory) macrophages, which are induced by proinflammatory mediators such as lipopolysaccharide (LPS) and Th1 cytokine interferon-γ; and M2, or "alternatively activated" (antiinflammatory) macrophages, which are generated in vitro by expo-

Original received February 23, 2009; revision received May 11, 2009; accepted May 20, 2009.

From the Department of Molecular Medicine and Metabolism (T.S., X.Y., Y.S., N.N., I.S., Y.K., Y.O.), Department of Biochemical Genetics (S.K.), Global Center of Excellence Program (Y.O.); and International Research Center for Molecular Science in Tooth and Bone Diseases, Laboratory of Recombinant Animals (T.U.), Medical Research Institute, Tokyo Medical and Dental University, Tokyo; Division of Biomedical Research Resources (K.U.-Y., J.M.), National Institute of Biomedical Innovation, Osaka; Kyoto Institute of Nutrition and Pathology (T.T., K.N.); Department of Medicine (Y.M.), Division of Atherosclerosis and Diabetes, National Cardiovascular Center Hospital, Osaka; and Department of Metabolic Disorder (K.Y.), Research Institute, International Medical Center of Japan, Tokyo, Japan.

Correspondence to Yoshihiro Ogawa, Department of Molecular Medicine and Metabolism, Medical Research Institute, Tokyo Medical and Dental University, 1-5-45 Yushima, Bunkyo-ku, Tokyo 113-8510, Japan. E-mail ogawa.mmm@mri.tmd.ac.jp

Circulation Research is available at http://circres.ahajournals.org

DOI: 10.1161/CIRCRESAHA.109.196261

sure to Th2 cytokines such as interleukin (IL)-4 and IL-13.[7–9] Evidence has accumulated indicating that macrophages, which are infiltrated into obese adipose tissue, exhibit the phenotypic change from M2 to M1 polarization.[7–9] Recent evidence also showed that the nuclear receptor peroxisome proliferator-activated receptor-γ or -δ regulates M2 polarization of adipose tissue macrophages and thus systemic insulin sensitivity.[8,9] It is, therefore, conceivable that M1 macrophages induce the release of saturated fatty acids from hypertrophied adipocytes via lipolysis, which, in turn, may serve as a proinflammatory adipocytokine locally in the adipose tissue.

Free fatty acids represent an important energy source mobilized from triglycerides stored in the adipose tissue, particularly during periods of starvation, but recent evidence has suggested the pathophysiologic roles other than the supply of nutrients in times of fasting or increased energy demand.[10] For instance, elevated levels of circulating free fatty acids, which are often associated with visceral fat obesity, increase fat accumulation in insulin target tissues such as the skeletal muscle and liver and contribute to insulin resistance.[11] We and others have reported that saturated fatty acids, which are released from adipocytes via the macrophage-induced lipolysis, serve as a naturally occurring ligand for Toll-like receptor (TLR)4 complex, which is essential for the recognition of LPS, to induce nuclear factor (NF)-κB activation in macrophages.[12–14] Evidence has also suggested that TLR4 plays an important role in adipose tissue inflammation.[14–17] Because macrophages in obese adipose tissue are exposed to saturated fatty acids released in large quantities from hypertrophied adipocytes, there might be negative regulatory mechanisms, whereby macrophages are protected against the saturated fatty acid–induced inflammatory response in obese adipose tissue.

Through a combination of cDNA microarray analyses of saturated fatty acid–stimulated macrophages in vitro and obese adipose tissue in vivo, we identified activating transcription factor (ATF)3, a member of the ATF/cAMP response element-binding protein (CREB) family of basic leucine zipper-type transcription factors[18,19] that is markedly induced in macrophages through TLR4 in response to saturated fatty acids in vitro and in obese adipose tissue in vivo. This study provides evidence that ATF3 acts as a transcriptional repressor of saturated fatty acids/TLR4 signaling in macrophages, thereby revealing the negative feedback mechanism that attenuates obesity-induced macrophage activation in obese adipose tissue. Our data also suggest that activation of ATF3 in macrophages offers a novel therapeutic strategy to prevent or treat obesity-induced inflammation and thus the metabolic syndrome associated with excess adiposity.

Materials and Methods

An expanded Materials and Methods section is available in the Online Data Supplement at http://circres.ahajournals.org.

Materials and Antibodies

Details are provided in the Online Data Supplement.

Animals

Six-week-old male C3H/HeJ mice, which have defective LPS signaling attributable to a missense mutation in the TLR4 gene,[20] and control C3H/HeN mice were purchased from CLEA Japan (Tokyo, Japan). Genetically obese *ob/ob*, *db/db*, and KKA^y mice were purchased from CLEA Japan and Charles River Japan (Tokyo, Japan). Details on experimental conditions are provided in the Online Data Supplement. All animal experiments were conducted in accordance to the guidelines of Tokyo Medical and Dental University Committee on Animal Research (No. 0090058).

Generation of Transgenic Mice Overexpressing ATF3 in Macrophages

Details are provided in the Online Data Supplement.

Cell Culture

RAW264 macrophage cell line (RIKEN BioResource Center, Tsukuba, Japan), 3T3-L1 preadipocytes, and HEK293 (American Type Culture Collection, Manassas, Va) were maintained in DMEM (Nacalai Tesque, Kyoto, Japan) containing 10% FBS (BioWest, Miami, Fla). Differentiation of 3T3-L1 preadipocytes to mature adipocytes was performed as previously described[6,12] and used as differentiated 3T3-L1 adipocytes at days 8 to 10 after the induction of differentiation. Murine peritoneal macrophages and bone marrow–derived macrophages were prepared as described.[12]

Chromatin Immunoprecipitation Assay

Details are provided in the Online Data Supplement.

Retrovirus-Mediated Overexpression and Knockdown of ATF3 in Macrophages

Retrovirus-mediated overexpression of the full-length mouse ATF3 cDNA and knockdown of endogenous ATF3 were performed in RAW264 macrophages as described in the Online Data Supplement.

Quantitative Real-Time PCR

Total RNA was extracted from cultured cells using Sepazol reagent (Nacalai Tesque) and quantitative real-time PCR was performed with an ABI Prism 7000 Sequence Detection System using PCR Master Mix Reagent (Applied Biosystems, Foster City, Calif).[6,12] Primers used in this study are described in Online Table I. Levels of mRNA were normalized to those of 36B4 mRNA.

Histological Analysis

Histological analysis was performed as previously described using the paraffin-embedded sections of the epididymal white adipose tissue.[15] In brief, hematoxylin/eosin staining was used to compare the adipocyte cell size with the software Win Roof (Mitani, Chiba, Japan).[15] The presence of F4/80-positive macrophages in the adipose tissue was detected immunohistochemically using the rat monoclonal antimouse F4/80 antibody[21] as described previously.[15] The number of F4/80-positive cells was counted in more than 10 mm^2 area of each section and expressed as the mean number/mm^2.

Western Blotting of ATF3

Whole cell lysates were prepared as previously described.[6] Samples (20 μg protein per lane) were separated by 12.5% SDS-PAGE and Western blotting was performed using antibodies against ATF3 (Santa Cruz Biotechnology).

Measurement of TNFα Levels in Culture Media

The TNFα levels in culture supernatants were determined by a commercially available ELISA kit (R&D systems, Minneapolis, Minn).[6]

Transient Transfection and Luciferase Assay

Details are provided in the Online Data Supplement.

Statistical Analysis

Data were expressed as the means±SE. Statistical analysis was performed using ANOVA, followed by Scheffe's test unless otherwise described. $P<0.05$ was considered to be statistically significant.

Results and Discussion

Identification of ATF3 As a Target Gene of Saturated Fatty Acids in Macrophages in Obese Adipose Tissue

We have provided in vitro evidence that saturated fatty acids, which are released from adipocytes via the macrophage-induced lipolysis, serves as a naturally occurring ligand that stimulates TLR4 signaling in macrophages.[12] To search for target gene(s) of saturated fatty acids in macrophages in obese adipose tissue, we performed cDNA microarray analysis of obese adipose tissue from *ob/ob* mice and palmitate-stimulated RAW264 macrophages (Online Figure I, a). Upregulated genes under both conditions included chemokines, proinflammatory cytokines, acute phase reactants, and ATF3 (Online Table II), whereas 5 genes were downregulated (Online Table III). ATF3 is a member of the ATF/CREB family of transcription factors.[18,19] ATF3 is rapidly induced in response to several stimuli and insults, such as chemicals, irradiation, and oxidative stress, and, in turn, negatively regulates target genes as a transcriptional repressor.[18,19] Although ATF3 plays a role in apoptosis and cell cycle,[18,19,22] the role of ATF3 in obesity is largely unknown. We, therefore, investigated the tissue distribution of ATF3 in obese and lean mice. Similar to macrophage marker F4/80, ATF3 mRNA expression was markedly increased in the adipose tissue from *db/db* mice relative to wild-type mice (Online Figure I, b). In this study, there was a significant increase in ATF3 mRNA expression in the liver from *db/db* mice relative to wild-type mice ($P<0.01$).

We confirmed our cDNA microarray data by real-time PCR and immunostaining. Expression of ATF3 and F4/80 mRNAs was increased in the adipose tissue during the course of diet-induced obesity (Figure 1A). We also observed upregulation of ATF3 and F4/80 in the adipose tissue from *ob/ob* mice (Figure 1B). Collagenase digestion of the adipose tissue, which is validated by F4/80 and adiponectin mRNA expression, revealed that ATF3 is expressed predominantly in stromal-vascular fraction in the adipose tissue (Figure 1C). Furthermore, ATF3 mRNA expression was increased significantly in *ob/ob* mice fed high-fat diet relative to wild-type mice fed standard diet ($P<0.01$) (Figure 1C). We also confirmed by immunostaining of ATF3 and F4/80 using serial sections of obese adipose tissue that most ATF3-positive cells are stained with F4/80 (Figure 1D). These observations indicate that ATF3 is markedly upregulated in obese adipose tissue, especially in infiltrated macrophages.

Saturated Fatty Acids Induce ATF3 via TLR4 in Macrophages In Vitro and In Vivo

We next examined the involvement of TLR4 in the saturated fatty acid–induced ATF3 mRNA and protein expression in macrophages in vitro. Saturated fatty acids, such as palmitate and stearate, and LPS increased significantly ATF3 mRNA and protein expression in RAW264 macrophages ($P<0.05$ versus vehicle) (Figure 2A through 2D). Interestingly, unsaturated fatty acids, such as oleate and eicosapentaenoic acid, did not affect ATF3 mRNA expression (Figure 2C and 2D and data not shown), suggesting the structure-specific effect of free fatty acids. We found that palmitate fails to increase ATF3 mRNA expression in peritoneal macrophages from C3H/HeJ mice with defective TLR4 signaling (Figure 2E). We also observed that BAY11-7085, an NF-κB inhibitor, markedly inhibits the palmitate-induced ATF3 mRNA expression in RAW264 macrophages (Figure 2F). The data were confirmed using RAW264 macrophages overexpressing a super-repressor form of IκBα (SR-IκBα) (Figure 2G). Furthermore, selective NF-κB activation by transient overexpression of p50 and p65 subunits of NF-κB increased significantly the ATF3 promoter activity in HEK293 cells ($P<0.01$) (Figure 2H). In this setting, the changes in ATF3 mRNA expression were almost parallel to those in TNFα mRNA expression (Figure 2E and 2F and data not shown). These observations indicate that TLR4/NF-κB pathway plays an important role in saturated fatty acid–induced ATF3 and TNFα expression in macrophages. On the other hand, palmitate and stearate, but not unsaturated fatty acids, are known to serve as precursors for de novo ceramide synthesis, thereby inducing inflammatory changes in certain cells.[23,24] However, we observed that pharmacological inhibition of ceramide synthesis slightly inhibits the palmitate-induced ATF3

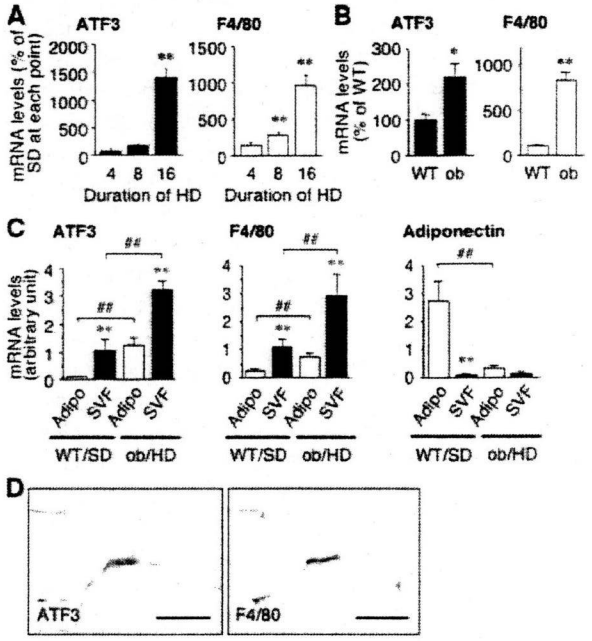

Figure 1. ATF3 expression in obese adipose tissue. ATF3 and F4/80 mRNA expression in the epididymal adipose tissue from high-fat diet (HD)-fed obese mice for up to 16 weeks (A) and genetically obese *ob/ob* mice at 15 weeks of age (ob) (B). *$P<0.05$, **$P<0.01$ vs standard diet (SD) or wild-type mice (WT) (n=6 to 10). C, ATF3, F4/80, and adiponectin mRNA expression in mature adipocytes (Adipo) and stromal-vascular fraction (SVF) in the epididymal adipose tissue from SD-fed WT and HD-fed ob. **$P<0.01$ vs the respective Adipo, ##$P<0.01$ (n=4 to 5). D, ATF3 and F4/80 immunostaining in the epididymal adipose tissue from HD-fed ob. Original magnification, ×400. Scale bars=100 μm.

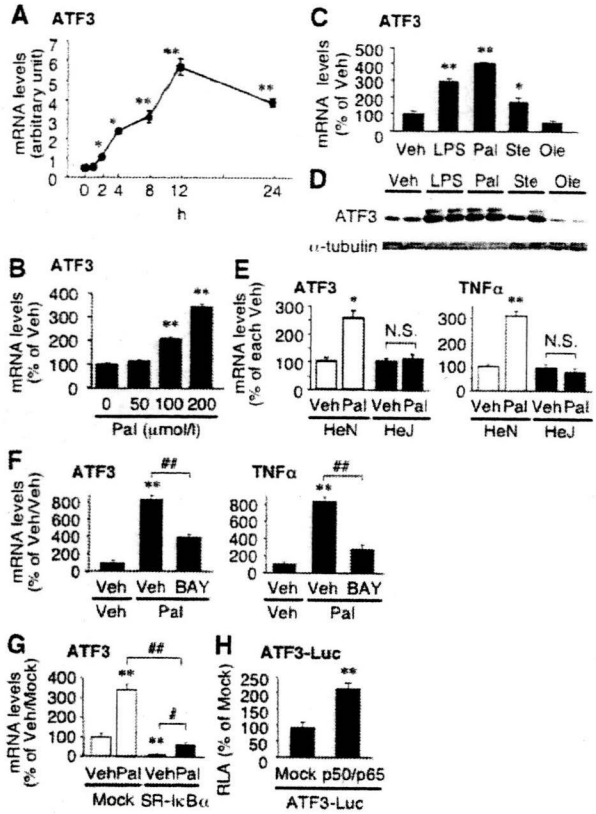

Figure 2. Saturated fatty acid–induced ATF3 expression in cultured macrophages. A, Time course of palmitate-induced ATF3 mRNA expression in RAW264 macrophages. Pal indicates palmitate 200 μmol/L. *$P<0.05$ vs 0 hour. B, Dose-dependent effect of palmitate on ATF3 mRNA expression in RAW264 macrophages. Effect of saturated and unsaturated fatty acids (FAs) on ATF3 mRNA (C) and protein (D) expression in RAW264 macrophages. Veh indicates vehicle; LPS, LPS 10 ng/mL; Pal, palmitate 200 μmol/L; Ste, stearate 200 μmol/L; Ole, oleate 200 μmol/L. *$P<0.05$, **$P<0.01$ vs Veh. E, Role of TLR4 in the palmitate-induced ATF3 and TNFα mRNA expression in peritoneal macrophages. HeN and HeJ indicate peritoneal macrophages from wild-type C3H/HeN and TLR4 mutant C3H/HeJ mice, respectively. *$P<0.05$, **$P<0.01$ vs Veh/HeN. F, Effect of NF-κB inhibitor BAY11-7085 (BAY, 10 μmol/L) on the palmitate-induced ATF3 and TNFα mRNA expression in RAW264 macrophages. **$P<0.01$ vs Veh/Veh, ##$P<0.01$. G, Effect of super-repressor IκBα (SR-IκBα) on the palmitate-induced ATF3 and TNFα mRNA expression in RAW264 macrophages. Mock and SR-IκBα, stably mock-, and SR-IκBα–expressing RAW264 macrophages, respectively. **$P<0.01$ vs Veh/mock; #$P<0.05$, ##$P<0.01$. H, Effect of NF-κB activation on ATF3 promoter activity. The luciferase reporter containing a 1.8-kb human ATF3 promoter fragment (ATF3-Luc) with p50 and p65 subunits of NF-κB or mock was transiently transfected in RAW264 macrophages. **$P<0.01$ vs mock (n=4 to 6).

mRNA expression in RAW264 macrophages (T. Suganami, I. Shirakawa, Y. Ogawa, unpublished data, 2009). These observations, taken together, suggest that saturated fatty acid–induced ATF3 expression is mediated mostly through the TLR4/NF-κB pathway.

We next examined the role of TLR4 in ATF3 expression in the interaction between adipocytes and macrophages. We have established an in vitro coculture system composed of adipocytes and macrophages and found that saturated fatty acids, which are released from adipocytes via the macrophage-induced lipolysis, are capable of activating the TLR4/NF-κB signaling.[6,12] Coculture of 3T3-L1 adipocytes with peritoneal macrophages from C3H/HeN mice resulted in the upregulation of ATF3 and TNFα mRNAs, which was significantly inhibited in the coculture with peritoneal macrophages from C3H/HeJ mice ($P<0.05$) (Online Figure II, a). We found that BAY11-7085 effectively inhibits the upregulation of ATF3 and TNFα mRNA expression in the coculture system (Online Figure II, b).

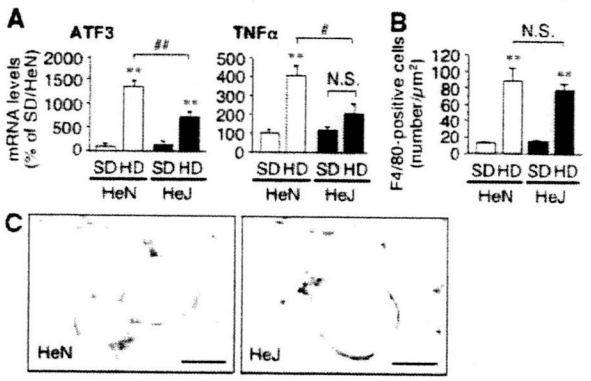

Figure 3. Role of TLR4 in obesity-induced ATF3 mRNA expression in adipose tissue macrophages. ATF3 and TNFα mRNA expression (A) and macrophage infiltration (B) in the adipose tissue from mice fed high-fat diet (HD) or standard diet (SD). **$P<0.01$ vs the respective SD; #$P<0.05$, ##$P<0.01$ (n=6 to 10). C, Immunostaining for ATF3 in the adipose tissue from HD-fed HeN and HeJ. Original magnification, ×400. Scale bars=100 μm.

Using C3H/HeJ and C3H/HeN mice fed high-fat diet, we also examined the involvement of TLR4 in obesity-induced ATF3 expression in the adipose tissue. There were no significant differences in body weight and adipose tissue weight between high-fat diet-fed C3H/HeN and C3H/HeJ mice (Online Table IV). Similar to our previous data on TNFα,[15] the high-fat diet–induced increase in ATF3 mRNA expression was significantly attenuated in the adipose tissue from C3H/HeJ mice relative to C3H/HeN mice ($P<0.01$) (Figure 3A). Importantly, there was no significant change in the number of macrophages infiltrated into the adipose tissue, as assessed by F4/80 immunostaining (Figure 3B), suggesting the attenuation of macrophage activation in C3H/HeJ mice. Immunohistochemical analysis also confirmed the marked reduction of ATF3 staining in C3H/HeJ mice relative to C3H/HeN mice during the high-fat diet (Figure 3C). Collectively, these observations suggest that the saturated fatty acid–induced ATF3 expression in macrophages is mediated via TLR4 in vitro and in vivo.

ATF3 Reduces Saturated Fatty Acid–Induced TNFα Production in Macrophages

To elucidate the functional role of ATF3 in macrophages, we examined the effect of ATF3 overexpression on proinflammatory cytokine production in macrophages in vitro. A full-length mouse ATF3 cDNA was stably overexpressed in RAW264 macrophages by retroviral transduction, which was confirmed by real-time PCR and Western blotting (Figure 4A). In RAW264 macrophages overexpressing ATF3 (ATF3-RAW264), the palmitate- and LPS-induced increase in TNFα

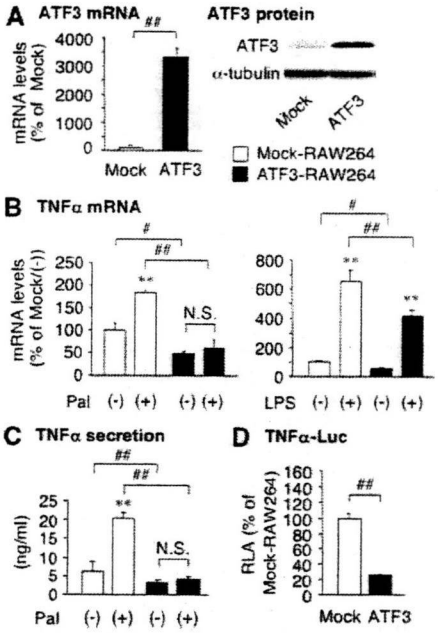

Figure 4. Effect of ATF3 overexpression on saturated fatty acid–induced TNFα production in cultured macrophages. A, Retrovirus-mediated stable overexpression of a full-length mouse ATF3 cDNA in RAW264 macrophages (ATF3-RAW264) and control RAW264 macrophages (Mock-RAW264). Effect of ATF3 overexpression on the palmitate- and LPS-induced TNFα mRNA expression (B) and secretion (C). D, Effect of ATF3 overexpression on the TNFα promoter activity. Pal indicates palmitate 200 μmol/L; LPS, LPS 10 ng/mL. $^{**}P<0.01$ vs the respective control; $\#P<0.05$, $\#\#P<0.01$ (n=4).

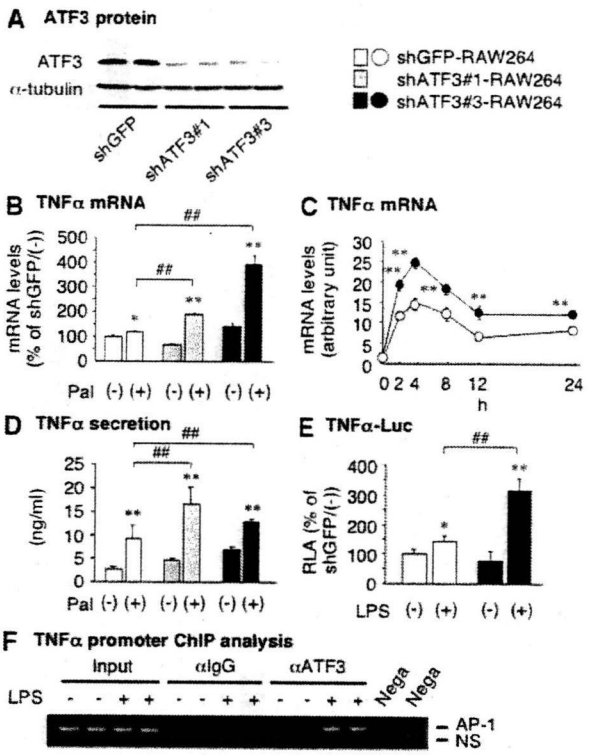

Figure 5. Effect of ATF3 knockdown on saturated fatty acid–induced TNFα production in cultured macrophages. A, Retrovirus-mediated ATF3 knockdown in RAW264 macrophages. Two short hairpin loop RNAs (shATF3#1 and shATF3#3) designed to target different sequences within ATF3 mRNA effectively knocked down endogenous ATF3 in RAW264 macrophages. B, Effect of ATF3 knockdown on the palmitate-induced TNFα mRNA expression. C, Time course of the LPS-induced TNFα mRNA expression in RAW264 macrophages. D, Effect of ATF3 knockdown on the palmitate-induced TNFα secretion. E, Effect of ATF3 knockdown on the TNFα promoter activity. shATF3#1-RAW264 and shATF3#3-RAW264 indicate ATF3–knocked-down RAW264 macrophages; shGFP-RAW264, control RAW264 macrophages; Pal, palmitate 200 μmol/L; LPS, LPS 10 ng/mL. $^{**}P<0.01$ vs the respective control; $\#P<0.05$, $\#\#P<0.01$ (n=4). F, TNFα promoter chromatin immunoprecipitation analysis with chromatin extracts prepared from RAW264 macrophages treated with or without LPS (100 ng/mL) for 6 hours. αATF3 indicates anti-ATF3 antibody; αIgG, normal rabbit IgG; Nega, negative control without template; NS, nonspecific band.

mRNA expression was significantly reduced relative to control RAW264 macrophages (Mock-RAW264) ($P<0.01$) (Figure 4B). We confirmed that the palmitate- and LPS-induced increase in TNFα secretion in the ATF3-RAW264 culture media is significantly reduced relative to Mock-RAW264 ($P<0.01$) (Figure 4C). We also observed with a luciferase reporter assay that TNFα promoter activity is markedly inhibited in ATF3-RAW264 relative to Mock-RAW264 (Figure 4D). Similarly, the palmitate-induced increase in IL-6 and inducible nitric oxide synthase was significantly reduced in ATF3-RAW264 relative to Mock-RAW264 (Online Figure III, a). These observations indicate that overexpression of ATF3 is capable of reducing the saturated fatty acid–induced proinflammatory cytokine production in macrophages.

We next examined the effect of knockdown of endogenous ATF3 gene expression in RAW264 macrophages. Stable knockdown of ATF3 using 2 independent short hairpin loop RNAs (shATF3#1 and shATF3#3) was confirmed by Western blotting (Figure 5A). The ATF3–knocked-down RAW264 macrophages (shATF3#1-RAW264 and shATF3#3-RAW264) exhibited significant enhancement of the palmitate-induced TNFα mRNA expression relative to control RAW264 macrophages (shGFP-RAW264) ($P<0.01$) (Figure 5B). The effect of ATF3 knockdown on TNFα mRNA expression persisted until 24 hours after stimulation with LPS (Figure 5C). Knockdown of ATF3 also significantly increased TNFα secretion in the culture media ($P<0.01$) (Figure 5D). Furthermore, we observed that the TNFα promoter activity is significantly increased in shATF3#3-RAW264 relative to shGFP-RAW264 ($P<0.01$) (Figure 5E). These observations suggest that once induced by the saturated fatty acids/TLR4 signaling, ATF3 attenuates the saturated fatty acid–induced TNFα production in macrophages, thereby constitute a negative feedback mechanism to reduce the TLR4 signaling induction of proinflammatory cytokine production. This notion is consistent with a recent report by Gilchrist et al that ATF3 acts as a negative regulator of the LPS-induced TLR4 signaling.[25]

In the proximal region of the IL-6 and IL-12b promoters, ATF3-binding ATF/CREB sites are located close to NF-κB binding sites.[25] NF-κB and ATF3, both of which are activated by saturated fatty acids/TLR4 signaling, can positively and negatively regulate their target proinflammatory cytokines, respectively.[25] However, there are no consensus sequences

corresponding to the ATF/CREB site close to the NF-κB–binding site (−534 bp) in the proximal region of TNFα promoter. In this study, we performed chromatin immunoprecipitation analysis with RAW264 macrophages and found that ATF3 is recruited to the region containing the activator protein (AP)-1 site (−926 bp) of the endogenous TNFα promoter (Figure 5F). This observation is consistent with a previous report that ATF3 binds to the AP-1 site.[26] It is, therefore, interesting to know how ATF3 negatively regulates TNFα and IL-6 production via its distinct binding sites: the AP-1 and ATF/CREB sites, respectively. In addition, histone deacetylase and heat shock transcription factor 1 are required for the action of ATF3 on the IL-6 promoter.[25,27] It is, therefore, important to identify ATF3-interacting proteins on the TNFα promoter.

Distinct Intracellular Signaling Pathways Plays a Role in the Palmitate- and LPS-Induced ATF3 Expression

In this study, we demonstrated that saturated fatty acids induce ATF3 expression in macrophages through the TLR4/NF-κB pathway, which is consistent with the previous report on LPS.[25] Besides NF-κB, mitogen-activated protein kinases (MAPKs) are an important intracellular signaling pathway downstream of TLR4,[28] and c-Jun N-terminal kinase (JNK) and p38 MAPK have been reported to play a role in ATF3 expression in certain cell types.[29,30] We, therefore, examined the involvement of MAPKs in the saturated fatty acid– and LPS-induced ATF3 mRNA expression and found that SB20358038, a p38 MAPK inhibitor, inhibits significantly the palmitate-induced ATF3 mRNA expression ($P<0.01$) (Online Figure IV). On the other hand, SP600125, a JNK inhibitor, inhibited most effectively the LPS-induced ATF3 mRNA expression ($P<0.01$) (Online Figure IV). Moreover, we found that ERK plays a major role in the palmitate-induced TNFα mRNA expression, whereas other MAPKs may also contribute to the LPS-induced TNFα mRNA expression (Online Figure IV). These observations, taken together, suggest that distinct intracellular signaling pathways may mediate the saturated fatty acid– and LPS-induced ATF3 mRNA expression through TLR4. It is interesting to know how endogenous and exogenous TLR4 ligands such as saturated fatty acids, oxidized phospholipids, and cytosolic and nuclear proteins, and LPS,[12,28,31] exert their effects through the unique signaling pathways, thereby leading to a variety of cellular responses.

Transgenic Overexpression of ATF3 Attenuates Macrophage Activation in Obese Adipose Tissue

To elucidate the role of ATF3 in macrophages infiltrated into obese adipose tissue, we developed transgenic mice overexpressing human ATF3 in macrophages under the control of SR-A promoter (ATF3 Tg) (Online Figure V, a).[32] Genomic Southern blot analysis identified 9 (line 2), 13 (line 25), and 20 (line 35) transgene copies in independent founder lines (data not shown). Western blot analysis of ATF3 revealed 3-fold and 2-fold increase in ATF3 protein levels in bone marrow–derived macrophages from lines 25 and 35, respectively, relative to wild-type mice (Online Figure V, b). In this study, there was no significant increase in ATF3 levels in line 2 macrophages (Online Figure V, b). We observed essentially the same data using peritoneal macrophages from 3 independent transgenic lines (Online Figure V, b).

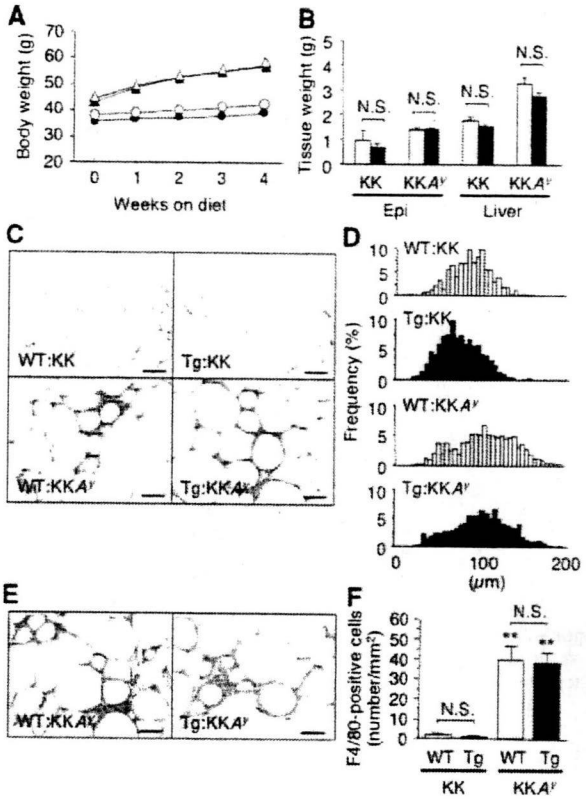

Figure 6. Adipocyte hypertrophy and macrophage infiltration in the adipose tissue from transgenic mice with macrophage-specific ATF3 overexpression. A, Time course of body weight. ○, WT:KK; ●, transgenic (Tg):KK; △, WT:KK*A*^{y}; ▲, Tg:KK*A*^{y}. B, The epididymal adipose tissue (Epi) and liver weights. Open bar, WT; closed bar, Tg. C, Hematoxylin/eosin staining of the epididymal adipose tissue. D, Histogram of diameters of adipocytes in the epididymal adipose tissue. E, F4/80 immunostaining of the epididymal adipose tissue. F, Cell count of F4/80-positive cells in the epididymal adipose tissue. $^{**}P<0.01$ vs the respective KK background (n=6 to 13).

We crossed ATF3 Tg (line 35) with genetically obese KK*A*^{y} mice and obtained 4 genotypes as the F1 generation (wild-type on the KK background [WT:KK], ATF3 Tg on the KK background [ATF3 Tg:KK], wild-type on the KK*A*^{y} background [WT:KK*A*^{y}], and ATF3 Tg on the KK*A*^{y} background [ATF3 Tg:KK*A*^{y}]) at a Mendelian ratio (data not shown). In this study, WT:KK and ATF3 Tg:KK were fed standard diet and WT:KK*A*^{y} and ATF3 Tg:KK*A*^{y} were fed high-fat diet for 4 weeks. During the course of high-fat diet feeding, transgenic overexpression of ATF3 in macrophages did not affect significantly body weight and epididymal fat weight on KK and KK*A*^{y} backgrounds (Figure 6A and 6B). The liver weight tended to be decreased in ATF3 Tg:KK*A*^{y} relative to WT:KK*A*^{y}, but the difference did not reach statistical significance (Figure 6B). Histological analysis showed no apparent difference in adipocyte cell size between genotypes (Figure 6C and 6D). There was no significant difference in obesity-induced macrophage infiltration be-

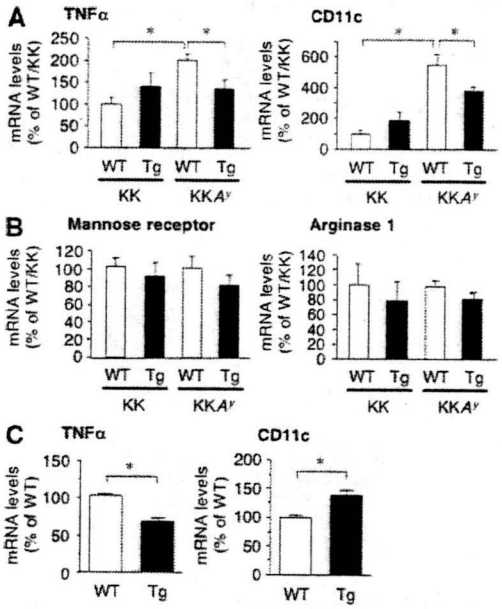

Figure 7. Effect of ATF3 on activation and polarization of adipose tissue macrophages and peritoneal macrophages from macrophage-specific ATF3 transgenic mice. A and B, mRNA expression of M1 markers (TNFα and CD11c) (A) and M2 markers (mannose receptor and arginase 1) (B) in the epididymal adipose tissue from WT:KK, Tg:KK, WT:KK*A*^{y}, and Tg:KK*A*^{y} mice. C, mRNA expression of M1 markers (TNFα and CD11c) in peritoneal macrophages from WT and Tg on the C57BL/6J background. *$P<0.05$ (n=6 to 13).

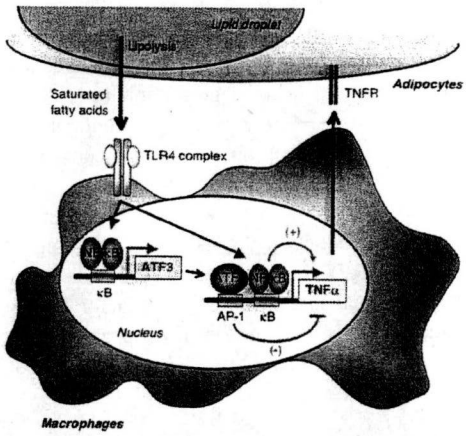

Figure 8. Negative feedback mechanism involving ATF3 as a transcriptional repressor of saturated fatty acid/TLR4 signaling in macrophages in obese adipose tissue. In the interaction between adipocytes and macrophages, ATF3 is upregulated in macrophages through the saturated fatty acids/TLR4/NF-κB signaling. Once induced, ATF3 can transcriptionally reduce the saturated fatty acids/TLR4 signaling–induced proinflammatory cytokine production. Our data have identified ATF3 as a transcriptional repressor of saturated fatty acid/TLR4 signaling, thereby revealing the negative feedback mechanism that attenuates macrophage activation in obese adipose tissue. TNFR indicates TNFα receptor; AP-1 and κB, AP-1– and NF-κB–binding elements, respectively.

tween WT:KK*A*^{y} and ATF3 Tg:KK*A*^{y} (Figure 6E and 6F). These observations suggest that transgenic overexpression of ATF3 in macrophages does not affect adipocyte hypertrophy and macrophage infiltration in obese adipose tissue.

We also examined the effect of ATF3 on macrophage activation and polarization in the adipose tissue from transgenic mice with macrophage-specific overexpression of ATF3. We observed a marked increase in TNFα mRNA expression in the adipose tissue from WT:KK*A*^{y} relative to WT:KK, which was significantly attenuated in ATF3 Tg:KK*A*^{y} ($P<0.05$) (Figure 7A). In this study, M1 macrophage marker CD11c was also increased in the adipose tissue from WT:KK*A*^{y} relative to WT:KK (Figure 7B), which was effectively inhibited in ATF3 Tg:KK*A*^{y} ($P<0.05$) (Figure 7A). Moreover, IL-6 mRNA expression tended to be decreased in the adipose tissue from ATF3 Tg:KK*A*^{y} mice relative to WT:KK*A*^{y} (Online Figure III, b). By contrast, we found no significant difference in mRNA expression of M2 macrophage markers, mannose receptor and arginase 1, among genotypes (Figure 7B). These observations suggest that overexpression of ATF3 in macrophages is capable of inhibiting macrophage activation and M1 polarization in the adipose tissue in vivo (Figure 8).

We next examined TNFα and CD11c mRNA expression in peritoneal macrophages prepared from ATF3 Tg and WT on the C57BL/6J background. Similar to the data on the adipose tissue (Figure 7A), TNFα mRNA expression was significantly suppressed in peritoneal macrophages from ATF3 Tg relative to WT ($P<0.05$) (Figure 7C). Interestingly, CD11c mRNA expression in peritoneal macrophages was rather higher in ATF3 Tg than in WT ($P<0.05$) (Figure 7C). In this regard, using ATF3-RAW264 and shATF3-RAW264, we did not observe that ATF3 has impact on CD11c mRNA expression in vitro (data not shown), suggesting that CD11c may not be a transcriptional target of ATF3 in macrophages. Further studies are needed to elucidate the role of ATF3 in obesity-induced M1 polarization of adipose tissue macrophages. Global ATF3-deficient mice are viable,[19,25] but the role of ATF3 in glucose/lipid metabolism has not been elucidated. Because activation and polarization of adipose tissue macrophages play an important role in the metabolic status,[7–9] studies with ATF3 Tg and macrophage-specific ATF3-deficient mice would help elucidate the pathophysiologic role of ATF3 in macrophages in adipose tissue inflammation and systemic glucose/lipid metabolism.

In conclusion, ATF3 is upregulated in macrophages in the interaction between adipocytes and macrophages through the saturated fatty acids/TLR4/NF-κB signaling. Once induced, ATF3 can transcriptionally reduce the saturated fatty acids/TLR4 signaling induction of proinflammatory cytokine production. Among known negative regulators of TLR4 signaling,[28] ATF3 is unique in that it represses the TLR4 target genes via a transcriptional mechanism. This study provides evidence that ATF3 acts as a transcriptional repressor of saturated fatty acids/TLR4 signaling, thereby revealing the negative feedback mechanism that attenuates macrophage activation in obese adipose tissue (Figure 8). Our data also suggest that activation of ATF3 in macrophages may offer a novel therapeutic strategy to prevent or treat obesity-induced adipose tissue inflammation.

Acknowledgments

We thank Ai Togo for secretarial assistance and Takanori Kunieda and Tae Mieda for technical assistance. We are also grateful to the members of the Ogawa laboratory for discussions.

Sources of Funding

This work was supported in part by a Grant-in-Aid for Scientific Research from the Ministry of Education, Culture, Sports, Science and Technology of Japan and Ministry of Health, Labor and Welfare of Japan and research grants from Takeda Science Foundation and Takeda Medical Research Foundation.

Disclosures

None.

References

1. Grundy SM, Brewer HB, Jr, Cleeman JI, Smith SC Jr, Lenfant C. Definition of metabolic syndrome: report of the National Heart, Lung, and Blood Institute/American Heart Association conference on scientific issues related to definition. *Circulation*. 2004;109:433–438.
2. Hotamisligil GS. Inflammation and metabolic disorders. *Nature*. 2006; 444:860–867.
3. Berg AH, Scherer PE. Adipose tissue, inflammation, and cardiovascular disease. *Circ Res*. 2005;96:939–949.
4. Matsuzawa Y, Funahashi T, Nakamura T. Molecular mechanism of metabolic syndrome X: contribution of adipocytokines adipocyte-derived bioactive substances. *Ann N Y Acad Sci*. 1999;892:146–154.
5. Weisberg SP, McCann D, Desai M, Rosenbaum M, Leibel RL, Ferrante AW Jr. Obesity is associated with macrophage accumulation in adipose tissue. *J Clin Invest*. 2003;112:1796–1808.
6. Suganami T, Nishida J, Ogawa Y. A paracrine loop between adipocytes and macrophages aggravates inflammatory changes: role of free fatty acids and tumor necrosis factor α. *Arterioscler Thromb Vasc Biol*. 2005; 25:2062–2068.
7. Lumeng CN, Bodzin JL, Saltiel AR. Obesity induces a phenotypic switch in adipose tissue macrophage polarization. *J Clin Invest*. 2007;117: 175–184.
8. Kang K, Reilly SM, Karabacak V, Gangl MR, Fitzgerald K, Hatano B, Lee CH. Adipocyte-derived Th2 cytokines and myeloid PPARδ regulate macrophage polarization and insulin sensitivity. *Cell Metab*. 2008;7: 485–495.
9. Odegaard JI, Ricardo-Gonzalez RR, Red Eagle A, Vats D, Morel CR, Goforth MH, Subramanian V, Mukundan L, Ferrante AW, Chawla A. Alternative M2 activation of Kupffer cells by PPARδ ameliorates obesity-induced insulin resistance. *Cell Metab*. 2008;7:496–507.
10. Cao H, Gerhold K, Mayers JR, Wiest MM, Watkins SM, Hotamisligil GS. Identification of a lipokine, a lipid hormone linking adipose tissue to systemic metabolism. *Cell*. 2008;134:933–944.
11. Unger RH. Lipotoxicity in the pathogenesis of obesity-dependent NIDDM. Genetic and clinical implications. *Diabetes*. 1995;44:863–870.
12. Suganami T, Tanimoto-Koyama K, Nishida J, Itoh M, Yuan X, Mizuarai S, Kotani H, Yamaoka S, Miyake K, Aoe S, Kamei Y, Ogawa Y. Role of the Toll-like receptor 4/NF-κB pathway in saturated fatty acid-induced inflammatory changes in the interaction between adipocytes and macrophages. *Arterioscler Thromb Vasc Biol*. 2007;27:84–91.
13. Lee JY, Sohn KH, Rhee SH, Hwang D. Saturated fatty acids, but not unsaturated fatty acids, induce the expression of cyclooxygenase-2 mediated through Toll-like receptor 4. *J Biol Chem*. 2001;276: 16683–16689.
14. Shi H, Kokoeva MV, Inouye K, Tzameli I, Yin H, Flier JS. TLR4 links innate immunity and fatty acid-induced insulin resistance. *J Clin Invest*. 2006;116:3015–3025.
15. Suganami T, Mieda T, Itoh M, Shimoda Y, Kamei Y, Ogawa Y. Attenuation of obesity-induced adipose tissue inflammation in C3H/HeJ mice carrying a Toll-like receptor 4 mutation. *Biochem Biophys Res Commun*. 2007;354:45–49.
16. Poggi M, Bastelica D, Gual P, Iglesias MA, Gremeaux T, Knauf C, Peiretti F, Verdier M, Juhan-Vague I, Tanti JF, Burcelin R, Alessi MC. C3H/HeJ mice carrying a Toll-like receptor 4 mutation are protected against the development of insulin resistance in white adipose tissue in response to a high-fat diet. *Diabetologia*. 2007;50:1267–1276.
17. Tsukumo DM, Carvalho-Filho MA, Carvalheira JB, Prada PO, Hirabara SM, Schenka AA, Araujo EP, Vassallo J, Curi R, Velloso LA, Saad MJ. Loss-of-function mutation in Toll-like receptor 4 prevents diet-induced obesity and insulin resistance. *Diabetes*. 2007;56:1986–1998.
18. Cai Y, Zhang C, Nawa T, Aso T, Tanaka M, Oshiro S, Ichijo H, Kitajima S. Homocysteine-responsive ATF3 gene expression in human vascular endothelial cells: activation of c-Jun NH_2-terminal kinase and promoter response element. *Blood*. 2000;96:2140–2148.
19. Hartman MG, Lu D, Kim ML, Kociba GJ, Shukri T, Buteau J, Wang X, Frankel WL, Guttridge D, Prentki M, Grey ST, Ron D, Hai T. Role for activating transcription factor 3 in stress-induced beta-cell apoptosis. *Mol Cell Biol*. 2004;24:5721–5732.
20. Poltorak A, He X, Smirnova I, Liu MY, Van Huffel C, Du X, Birdwell D, Alejos E, Silva M, Galanos C, Freudenberg M, Ricciardi-Castagnoli P, Layton B, Beutler B. Defective LPS signaling in C3H/HeJ and C57BL/10ScCr mice: mutations in TLR4 gene. *Science*. 1998;282:2085–2088.
21. Kitagawa K, Wada T, Furuichi K, Hashimoto H, Ishiwata Y, Asano M, Takeya M, Kuziel WA, Matsushima K, Mukaida N, Yokoyama H. Blockade of CCR2 ameliorates progressive fibrosis in kidney. *Am J Pathol*. 2004;165:237–246.
22. Tamura K, Hua B, Adachi S, Guney I, Kawauchi J, Morioka M, Tamamori-Adachi M, Tanaka Y, Nakabeppu Y, Sunamori M, Sedivy JM, Kitajima S. Stress response gene ATF3 is a target of c-myc in serum-induced cell proliferation. *EMBO J*. 2005;24:2590–2601.
23. Shulman GI. Cellular mechanisms of insulin resistance. *J Clin Invest*. 2000;106:171–176.
24. Haversen L, Danielsson KN, Fogelstrand L, Wiklund O. Induction of proinflammatory cytokines by long-chain saturated fatty acids in human macrophages. *Atherosclerosis*. 2009;202:382–393.
25. Gilchrist M, Thorsson V, Li B, Rust AG, Korb M, Roach JC, Kennedy K, Hai T, Bolouri H, Aderem A. Systems biology approaches identify ATF3 as a negative regulator of Toll-like receptor 4. *Nature*. 2006;441:173–178.
26. Kim HB, Kong M, Kim TM, Suh YH, Kim WH, Lim JH, Song JH, Jung MH. NFATc4 and ATF3 negatively regulate adiponectin gene expression in 3T3-L1 adipocytes. *Diabetes*. 2006;55:1342–1352.
27. Inouye S, Fujimoto M, Nakamura T, Takaki E, Hayashida N, Hai T, Nakai A. Heat shock transcription factor 1 opens chromatin structure of interleukin-6 promoter to facilitate binding of an activator or a repressor. *J Biol Chem*. 2007;282:33210–33217.
28. Akira S, Takeda K. Toll-like receptor signalling. *Nat Rev Immunol*. 2004;4:499–511.
29. Lim JH, Lee JI, Suh YH, Kim W, Song JH, Jung MH. Mitochondrial dysfunction induces aberrant insulin signalling and glucose utilisation in murine C2C12 myotube cells. *Diabetologia*. 2006;49:1924–1936.
30. Lu D, Chen J, Hai T. The regulation of ATF3 gene expression by mitogen-activated protein kinases. *Biochem J*. 2007;401:559–567.
31. Imai Y, Kuba K, Neely GG, Yaghubian-Malhami R, Perkmann T, van Loo G, Ermolaeva M, Veldhuizen R, Leung YH, Wang H, Liu H, Sun Y, Pasparakis M, Kopf M, Mech C, Bavari S, Peiris JS, Slutsky AS, Akira S, Hultqvist M, Holmdahl R, Nicholls J, Jiang C, Binder CJ, Penninger JM. Identification of oxidative stress and Toll-like receptor 4 signaling as a key pathway of acute lung injury. *Cell*. 2008;133:235–249.
32. Horvai A, Palinski W, Wu H, Moulton KS, Kalla K, Glass CK. Scavenger receptor A gene regulatory elements target gene expression to macrophages and to foam cells of atherosclerotic lesions. *Proc Natl Acad Sci U S A*. 1995;92:5391–5395.

OBSERVATIONS

Unbalanced M1/M2 Phenotype of Peripheral Blood Monocytes in Obese Diabetic Patients

Effect of pioglitazone

The monocyte-macrophage system exists in at least two distinct phenotypes of differentiation: proinflammatory (M1) and anti-inflammatory (M2) (1,2). Macrophages, when infiltrated into obese adipose tissue, exhibit a phenotypic switch from M2 to M1 polarization, thereby contributing to obesity-induced adipose tissue inflammation and insulin resistance (1). Expression of both M1 and M2 markers is detected in circulating peripheral blood mononuclear cells as well as in atherosclerotic plaques (3). However, there have been no detailed studies on the M1/M2 phenotype of monocytes and their association with cardiovascular risks in obese subjects with type 2 diabetes. On the other hand, we demonstrated that pioglitazone, a thiazolidinedione class of insulin sensitizer, exerts an antiatherogenic effect independent of its antidiabetic effect (4). Here, we investigated the M1/M2 phenotype of peripheral blood monocytes and pulse wave velocity (PWV), an established index of arterial stiffness, and also the effect of pioglitazone in obese diabetic patients.

A total of 161 subjects (95 men and 66 women, mean age 50.4 years), including 45 normal-weight control subjects, 62 obese nondiabetic patients, and 54 obese diabetic patients with or without pioglitazone treatment for 3 months (30 mg daily), were recruited in our clinic. Peripheral blood monocytes were prepared using magnetic-assisted cell sorting and flow cytometry with anti-CD14. Expression of M1/M2 markers was analyzed by real-time quantitative PCR method and flow cytometry. The number and percentage of $CD14^+$ cells among peripheral blood monocytes from obese diabetic patients were significantly increased relative to those of control subjects ($P < 0.05$). The $CD14^+$ cells from obese nondiabetic patients showed significantly higher expression of M1 markers, tumor necrosis factor-α, and interleukin (IL)-6 and lower expression of an M2 marker, IL-10, relative to control subjects ($P < 0.01$). This is consistent with a report that peripheral blood mononuclear cells in obesity are in an inflammatory state (5). In addition, expression of IL-10 and CD163 in $CD14^+$ cells from obese diabetic patients was significantly decreased relative to that of obese nondiabetic patients ($P < 0.01$). Multivariate regression analysis showed that expression of tumor necrosis factor-α is independently associated with age and BMI and that expression of IL-6 is independently associated with BMI and LDL cholesterol ($P < 0.01$); expression of IL-10 was negatively and independently associated with diastolic blood pressure, A1C, and triglycerides, and expression of CD163 was negatively and independently associated with insulin concentration, A1C, and PWV ($P < 0.05$). Moreover, only age and CD163 were independently correlated with PWV ($P < 0.05$). Interestingly, 3-month treatment with pioglitazone significantly increased IL-10 and CD163 and decreased IL-6 ($P < 0.05$) in parallel with the improvement of fasting plasma glucose, A1C, insulin concentration, homeostasis model assessment-insulin resistance index, and PWV in obese diabetic patients. Further studies are required to elucidate more detailed characterization of monocyte subsets in obese diabetic patients and the resulting pathophysiological implication in cardiovascular diseases.

This study provides evidence that an unbalanced M1/M2 phenotype of peripheral blood monocytes is associated with metabolic disorder and arterial stiffness in obese type 2 diabetic patients. We also demonstrate that peroxisome proliferator–activated receptor-γ activation improves the unbalanced M1/M2 phenotype of monocytes in obese diabetic patients, which may contribute to its antiatherogenic effect.

NORIKO SATOH, MD, PHD[1]
AKIRA SHIMATSU, MD, PHD[1]
AKIHIRO HIMENO, MD[1,2]
YOUSUKE SASAKI, BSC[1]
HAJIME YAMAKAGE, BSC[1]
KAZUNORI YAMADA, MD, PHD[2]
TAKAYOSHI SUGANAMI, MD, PHD[3]
YOSHIHIRO OGAWA, MD, PHD[3,4]

From the [1]Clinical Research Institute for Endocrine Metabolic Diseases, National Hospital Organization, Kyoto Medical Center, Kyoto, Japan; the [2]Diabetes Center, National Hospital Organization, Kyoto Medical Center, Kyoto, Japan; the [3]Department of Molecular Medicine and Metabolism, Medical Research Institute, Tokyo Medical and Dental University, Tokyo, Japan; and the [4]Global Center of Excellence Program, International Research Center for Molecular Science in Tooth and Bone Diseases, Tokyo Medical and Dental University, Tokyo, Japan.

Corresponding author: Noriko Satoh, nsato@kyotolan.hosp.go.jp.

DOI: 10.2337/dc09-1315

Acknowledgments— This work was supported in part by a Grant-in-Aid for Scientific Research from the Ministry of Education, Culture, Sports, Science and Technology of the Japan Ministry of Health, Labor, and Welfare of Japan (to N.S. and Y.O.), the Smoking Research Foundation (to N.S.), and Takeda Science Foundation (to Y.O.).

No other potential conflicts of interest relevant to this article were reported.

References

1. Lumeng CN, Bodzin JL, Saltiel AR. Obesity induces a phenotypic switch in adipose tissue macrophage polarization. J Clin Invest 2007;117:175–184
2. Gordon S, Taylor PR. Monocyte and macrophage heterogeneity. Nat Rev Immunol 2005;5:953–964
3. Bouhlel MA, Derudas B, Rigamonti E, Dièvart R, Brozek J, Haulon S, Zawadzki C, Jude B, Torpier G, Marx N, Staels B, Chinetti-Gbaguidi G. PPARγ activation primes human monocytes into alternative M2 macrophages with anti-inflammatory properties. Cell Metab 2007;6:137–143
4. Satoh N, Ogawa Y, Usui T, Tagami T, Kono S, Uesugi H, Sugiyama H, Sugawara A, Yamada K, Shimatsu A, Kuzuya H, Nakao K. Antiatherogenic effect of pioglitazone in type 2 diabetic patients irrespective of the responsiveness to its antidiabetic effect. Diabetes Care 2003;26:2493–2499
5. Ghanim H, Aljada A, Hofmeyer D, Syed T, Mohanty P, Dandona P. Circulating mononuclear cells in the obese are in a proinflammatory state. Circulation 2004;110:1564–1571

Insulin-Induced Ectodomain Shedding of Heparin-Binding Epidermal Growth Factor-Like Growth Factor in Adipocytes *In Vitro*

Takanobu Yamamoto[1,2], Takayoshi Suganami[1], Minako Kiso-Narita[1], Peggy A. Scherle[3], Yasutomi Kamei[1], Mitsuaki Isobe[2], Shigeki Higashiyama[4] and Yoshihiro Ogawa[1,5]

Heparin-binding epidermal growth factor-like growth factor (HB-EGF) is synthesized as a type I transmembrane protein, which is proteolytically cleaved to release a soluble form via members of the a disintegrin and metalloproteinase (ADAM) family of proteolytic enzymes. This study was designed to elucidate the molecular mechanism underlying insulin-induced HB-EGF shedding in adipocytes *in vitro*. The 3T3-L1 adipocytes with stable expression of alkaline phosphatase (AP)-tagged proHB-EGF (3T3-L1/HB-EGF-AP adipocytes) were developed and AP activities of conditioned media were determined. Using 3T3-L1/HB-EGF-AP adipocytes, we demonstrated that insulin induces HB-EGF shedding in differentiated 3T3-L1 adipocytes in a dose- and time-dependent manner. There is no significant increase in insulin-induced HB-EGF shedding in undifferentiated 3T3-L1 preadipocytes. Studies with metalloprotease inhibitors suggested that insulin-induced HB-EGF shedding in adipocytes is mediated at least in part via ADAM17. Treatment with recombinant HB-EGF results in a dose- and time-dependent increase in HB-EGF shedding in adipocytes, which is significantly suppressed by pharmacologic blockade of ADAM17 ($P < 0.01$). Moreover, insulin-induced HB-EGF shedding in adipocytes is significantly inhibited by AG1478, an EGF receptor antagonist ($P < 0.01$). This study provides *in vitro* evidence that insulin induces HB-EGF shedding in 3T3-L1 adipocytes. Our data also suggest the role of ADAM17 in insulin-induced HB-EGF shedding in adipocytes.

Obesity (2010) doi:10.1038/oby.2010.2

INTRODUCTION

The adipose tissue secretes a large number of adipocytokines such as leptin, monocyte chemoattractant protein-1, and adiponectin, which may be involved in a variety of physiologic and pathologic conditions (1). Unbalanced production of pro- and anti-inflammatory adipocytokines seen in visceral fat obesity critically contributes to the development of many aspects of the metabolic syndrome (1,2). Recently, we have demonstrated that a paracrine loop involving saturated free fatty acids and tumor necrosis factor-α (TNFα) derived from adipocytes and macrophages, respectively, establishes a vicious cycle that aggravates the inflammatory changes in obese adipose tissue (3,4), suggesting that adipocytokine production by hypertrophied adipocytes during obesity is influenced by the presence of infiltrating macrophages, through mutual crosstalk. On the other hand, hyperinsulinemia as a result of obesity-induced insulin resistance may also play a role in the alteration of adipocytokine production.

There are at least two classical secretory pathways in a variety of cell types, regulated vs. constitutive pathways (5). However, there is no direct evidence to support the presence of regulated secretory pathway in lipid-laden mature adipocytes. Indeed, most adipocytokines are thought to be secreted from mature adipocytes with a small capacity of storage via the constitutive pathway (6). On the other hand, there are numerous proteolytic enzymes expressed in adipocytes *in vitro* or in the adipose tissue *in vivo* (7,8), suggesting that proteolytic cleavage and release of membrane proteins is also a crucial regulatory step in mature adipocytes.

Heparin-binding epidermal growth factor-like growth factor (HB-EGF) plays a major role in wound healing, tumor growth, and cardiovascular diseases via endocrine, paracrine, or autocrine mechanisms (9,10). Like other members of the EGF family, HB-EGF is synthesized as a type I transmembrane protein (proHB-EGF) that undergoes proteolytic cleavage to release a

[1]Department of Molecular Medicine and Metabolism, Medical Research Institute, Tokyo Medical and Dental University, Tokyo, Japan; [2]Department of Cardiovascular Medicine, Graduate School of Medicine, Tokyo Medical and Dental University, Tokyo, Japan; [3]Drug Discovery, Incyte Corporation, Wilmington, Delaware, USA; [4]Department of Biochemistry and Molecular Genetics, Ehime University Graduate School of Medicine, Ehime, Japan; [5]Global Center of Excellence Program; International Research Center for Molecular Science in Tooth and Bone Diseases, Medical Research Institute, Tokyo Medical and Dental University, Tokyo, Japan. Correspondence: Yoshihiro Ogawa (ogawa.mmm@mri.tmd.ac.jp)

Received 20 May 2009; accepted 5 January 2010; advance online publication 28 January 2010. doi:10.1038/oby.2010.2

soluble growth factor. The "ectodomain shedding" of HB-EGF, which is essential to transactivate EGF receptor, is mediated via members of the a disintegrin and metalloproteinase (ADAM) family of proteolytic enzymes called sheddases (10). Ectodomain shedding of HB-EGF is induced by multiple stimuli such as phorbol 12-myristate 13-acetate, calcium ionophore, and various growth factors and cytokines (10). There are a couple of reports demonstrating that HB-EGF is present in the systemic circulation (11,12). Matsumoto *et al.* reported previously that HB-EGF mRNA is expressed abundantly in the mouse and human adipose tissue and that plasma HB-EGF concentrations are elevated in proportion to the degree of adiposity in humans or in obese patients with coronary artery disease (12). There are also a couple of reports showing that several ADAMs and matrix metalloproteinases (MMPs) known to induce HB-EGF shedding are expressed in the adipose tissue (7,8). Toward understanding the physiologic and pathophysiologic role of HB-EGF as an adipocytokine, it is important to know the regulatory mechanism of HB-EGF shedding in adipocytes.

Here, we provide *in vitro* evidence that insulin induces HB-EGF shedding in 3T3-L1 adipocytes. Our data also suggest the role of ADAM17/TNFα-converting enzyme in insulin-induced HB-EGF shedding in adipocytes.

METHODS AND PROCEDURES

Materials and animals

Details on materials and animal experiments are in **Supplementary Methods and Procedures** online. All animal experiments were conducted according to the guidelines of Tokyo Medical and Dental University Committee on Animal Research (No. 0060026).

Cell culture

The 3T3-L1 preadipocytes (American Type Culture Collection, Manassas, VA) were maintained in Dulbecco's modified Eagle's medium containing 10% fetal bovine serum (BioWest, Miami, FL). Differentiation of 3T3-L1 preadipocytes to adipocytes was described elsewhere (13).

Development of 3T3-L1 adipocytes stably expressing AP-tagged proHB-EGF

The 3T3-L1 adipocytes with stable expression of alkaline phosphatase (AP)-tagged proHB-EGF (3T3-L1/HB-EGF-AP adipocytes) were developed as follows. The HB-EGF-AP retroviral expression vector was constructed by inserting the *Hind*III-*Xba*I fragment of pSS-AIPh/HB-EGF encoding AP-tagged HB-EGF (14) into pRMX-IRES-Puro vector (15), and transfected into Plat-E packaging cells (16) using Lipofectamine 2000 (Invitrogen Life Technologies, Carlsbad, CA) according to the manufacturer's instructions. Viral supernatants were harvested from 24 to 48 h after transfection and applied to 3T3-L1 preadipocytes in Dulbecco's modified Eagle's medium containing 10% fetal bovine serum and 5 μg/ml of polybrene in a final volume of 5 ml. The 3T3-L1/HB-EGF-AP adipocytes were selected by 2 μg/ml of puromycin. In this study, there was no obvious difference in lipid accumulation between 3T3-L1/HB-EGF-AP and 3T3-L1 adipocytes during the course of adipocyte differentiation (data not shown). Expression of mRNAs for adipocyte markers (glucose transporter 4, adiponectin, and adipocyte fatty acid-binding protein) was increased after differentiation (see **Supplementary Figure S1** online).

HB-EGF-AP shedding assay

The 3T3-L1/HB-EGF-AP adipocytes were seeded and cultured in 6-well plates. Aliquots (200 μl) of conditioned media were heated for 10 min at 65 °C to inactivate endogenous APs and then 50 μl was transferred to 96-well plates. An equal volume of 2 × AP buffer (2 mol/l diethanolamine, pH 9.8, 1 mmol/l $MgCl_2$, 20 mmol/l L-homoarginine, and 24 mmol/l p-nitrophenylphosphate) was added to each well and gently mixed at room temperature until color development was apparent in positive control wells. AP activity was determined by measurement of absorbance at 405 nm with a microplate reader (14).

Measurement of 2-[^{3}H] deoxy-D-glucose uptake and triglyceride content

Basal and insulin-induced 2-deoxyglucose uptake and triglyceride content in 3T3-L1 adipocytes was measured as reported (13).

Quantitative real-time PCR

Quantitative real-time PCR was performed as described (3). Primers used for quantitative real-time PCR were described in **Table 1**. Levels of mRNA were normalized to those of 36B4 mRNA.

Statistical analysis

Data were expressed as means ± s.e. Statistical analysis was performed using ANOVA followed by Scheffe's test. $P < 0.05$ was considered to be statistically significant.

Table 1 Primers used for quantitative real-time PCR

Genes		Primers
HB-EGF	Forward	5′-TGCTGAAGCTCTTTCTGGCC-3′
	Reverse	5′-GAAGCCGCTCCAGACTCTCA-3′
adiponectin	Forward	5′-ATGGCAGAGATGGCACTCCT-3′
	Reverse	5′-CCTTCAGCTCCTGTCATTCCA-3′
aP2	Forward	5′-AGCATCATAACCCTAGATGGCG-3′
	Reverse	5′-CATAACACATTCCACCACCAGC-3′
Glut4	Forward	5′-CTGCAAAGCGTAGGTACCAA-3′
	Reverse	5′-CCTCCCGCCCTTAGTTG-3′
MMP3	Forward	5′-TCAGTCCCTCTATGGAACTCCC-3′
	Reverse	5′-CAGAGAGTTAGACTTGGTGGG TACC-3′
ADAM9	Forward	5′-CCAGACCCAGGGATGGTGAAT-3′
	Reverse	5′-GGCCATGACATTTTCCCTGAA-3′
ADAM10	Forward	5′-GCCAGCCTATCTGTGGAAACGGG-3′
	Reverse	5′-TTAGCGTCGCATGTGTCCCATTTG-3′
ADAM12	Forward	5′-GAGTGTGACTGCGGAGAACCGGAG GAA-3′
	Reverse	5′-ATTTTCCCACACTTGGCATCTCTCA-3′
ADAM17	Forward	5′-GCGGCGTCTCCTCATCCT-3′
	Reverse	5′-TTATATTCTGCCCCATCTGTG TTG-3′
MCP-1	Forward	5′-CCACTCACCTGCTGCTACTCAT-3′
	Reverse	5′-TGGTGATCCTCTTGTAGCTCTCC-3′
IL-6	Forward	5′-ACAACCACGGCCTTCCCTACTT-3′
	Reverse	5′-CACGA TTTCC CAGAG AACAT GTG-3′
36B4	Forward	5′-GGCCCTGCACTCTCGCTTTC-3′
	Reverse	5′-TGCCAGGACGCGCTTGT-3′

ADAM, a disintegrin and metalloproteinase; aP2, adipocyte fatty acid-binding protein; Glut4, glucose transporter 4; HB-EGF, heparin-binding epidermal growth factor-like growth factor; IL-6, interleukin 6; MCP-1, monocyte chemoattractant protein-1; MMP, matrix metalloproteinase.

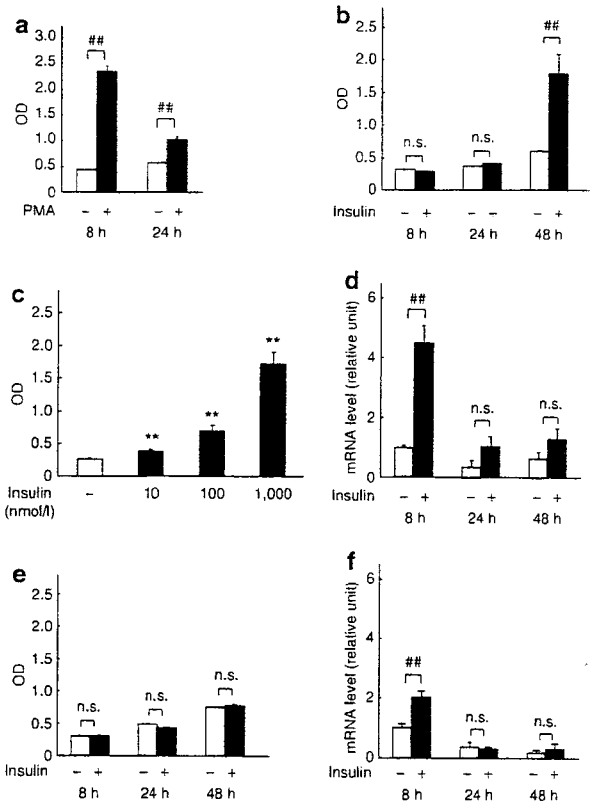

Figure 1 Effect of insulin on HB-EGF shedding and mRNA expression in 3T3-L1 adipocytes. (**a**) Time course of HB-EGF shedding in differentiated 3T3-L1/HB-EGF-AP adipocytes treated with PMA. Optical density (OD) shows the absorbance at 405 nm, which indicates AP activity in the conditioned media. Open bars, vehicle; filled bars, PMA (100 nmol/l). (**b**) Time course of HB-EGF shedding in differentiated 3T3-L1/HB-EGF-AP adipocytes treated with insulin. Open bars, vehicle; filled bars, insulin (100 nmol/l). (**c**) Dose response of insulin-induced HB-EGF shedding in 3T3-L1/HB-EGF-AP adipocytes treated with insulin for 48 h. Open bar, vehicle; filled bars, insulin with indicated doses. (**d**) Time course of insulin-induced HB-EGF mRNA expression in 3T3-L1 adipocytes treated with insulin. Open bars, vehicle; filled bars, insulin (100 nmol/l). (**e**) Time course of HB-EGF shedding in undifferentiated 3T3-L1/HB-EGF-AP preadipocytes treated with insulin. Open bars, vehicle; filled bars, insulin (100 nmol/l). (**f**) Time course of HB-EGF mRNA expression in undifferentiated 3T3-L1 preadipocytes treated with insulin. Open bars, vehicle; filled bars, insulin (100 nmol/l). $^{**}P < 0.01$ vs. vehicle. $^{\#\#}P < 0.01$. $n = 4$–6. AP, alkaline phosphatase; HB-EGF, heparin-binding epidermal growth factor-like growth factor; n.s., not significant; PMA, phorbol 12-myristate 13-acetate; 3T3-L1/HB-EGF-AP, 3T3-L1 with stable expression of AP-tagged proHB-EGF.

RESULTS

Expression of HB-EGF mRNA in the adipose tissue from rodent models of obesity

We found that HB-EGF mRNA expression is high in the adipose tissue from insulin-resistant animals (see **Supplementary Figure S2** online). HB-EGF mRNA expression was markedly increased in the subcutaneous and parametrial adipose tissue from 22-week-old female db/db mice fed a high-fat diet relative to age- and sex-matched control lean mice fed a standard diet (subcutaneous: $P < 0.05$; parametrial: $P < 0.01$) (see **Supplementary Figure S2a** online). We also observed that HB-EGF mRNA expression is increased in the subcutaneous and epididymal adipose tissue from 22-week-old male ob/ob mice relative to age- and sex-matched control lean littermates ($P < 0.05$) (see **Supplementary Figure S2b** online). In addition, we observed increased HB-EGF mRNA expression in 22-week-old male C3H/HeN mice fed a high-fat diet for 16 weeks relative to those fed a standard diet ($P < 0.01$) (see **Supplementary Figure S2c** online). Collagenase digestion of the adipose tissue from db/db mice fed a high-fat diet, which was validated by adiponectin mRNA expression, as an adipocyte marker, and F4/80 mRNA expression, as a macrophage marker, revealed significant amount of HB-EGF mRNA in both the adipocyte and stromal-vascular fractions. With a macrophage marker F4/80 expressed in both fractions, this is most likely accounted for by macrophages that commonly adhere to adipocytes (see **Supplementary Figure S3** online).

Development of 3T3-L1/HB-EGF-AP adipocytes

Because immunoassays with which to measure soluble HB-EGF immunoreactivity in mice are currently unavailable, we developed 3T3-L1/HB-EGF-AP adipocytes to make quantitative assessment of HB-EGF shedding in adipocytes *in vitro*. In this study, we confirmed that phorbol 12-myristate 13-acetate, which is known to induce HB-EGF shedding (17), at a dose of 100 nmol/l induces the release of HB-EGF-AP activity in differentiated 3T3-L1 adipocytes (**Figure 1a**). These observations suggest that 3T3-L1/HB-EGF-AP adipocytes are the useful experimental system to investigate the regulatory mechanism of HB-EGF shedding in adipocytes *in vitro*.

Effect of insulin on HB-EGF shedding in 3T3-L1 adipocytes

Using 3T3-L1/HB-EGF-AP adipocytes, we examined the effect of insulin on HB-EGF shedding in adipocytes. Treatment with insulin significantly induced HB-EGF shedding in 3T3-L1/HB-EGF-AP adipocytes 8 days after the differentiation, thus reaching up to approximately threefold relative to vehicle-treated groups 48 h after the treatment ($P < 0.01$) (**Figure 1b**). Insulin also increased HB-EGF shedding dose-dependently (10–1,000 nmol/l) (**Figure 1c**). In this study, we found that insulin increases significantly HB-EGF mRNA expression in differentiated 3T3-L1 adipocytes relative to vehicle-treated groups 8 h after the treatment ($P < 0.01$) (**Figure 1d**). However, there was no significant difference in HB-EGF mRNA expression between insulin- and vehicle-treated groups 24 and 48 h after the treatment.

We found that insulin does not induce HB-EGF shedding in undifferentiated 3T3-L1/HB-EGF-AP preadipocytes (**Figure 1e**). Treatment with insulin increased significantly HB-EGF mRNA expression in undifferentiated 3T3-L1 preadipocytes 8 h after the treatment ($P < 0.01$) (**Figure 1f**).

Effect of mitogen-activated protein kinase/extracellular signal-regulated kinase and phosphoinositide 3-kinase inhibitors on insulin-induced HB-EGF shedding in 3T3-L1 adipocytes

Several ADAMs, which are responsible for HB-EGF shedding, are known to be activated via the mitogen-activated protein

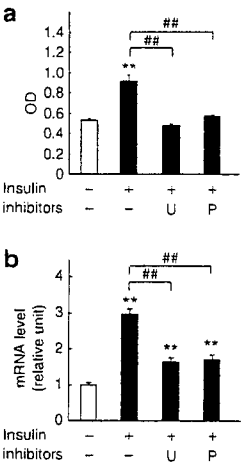

Figure 2 Effect of MEK inhibitors on insulin-induced HB-EGF shedding and mRNA expression in 3T3-L1 adipocytes. (**a**) Effect of MEK inhibitors on HB-EGF shedding in differentiated 3T3-L1/HB-EGF-AP adipocytes treated with insulin for 48 h. Optical density (OD) shows the absorbance at 405 nm, which indicates AP activity in the conditioned media. Open bar, vehicle; filled bars, insulin (100 nmol/l) with or without inhibitors. (**b**) Effect of MEK inhibitors on HB-EGF mRNA expression in 3T3-L1 adipocytes treated with insulin for 8 h. Open bar, vehicle; filled bars, insulin (100 nmol/l) with or without inhibitors. U, U0126 (10 μmol.l); P, PD98059 (50 μmol/l). $^{**}P < 0.01$ vs. vehicle. $^{\#\#}P < 0.01$. $n = 4$–6. AP, alkaline phosphatase; HB-EGF, heparin-binding epidermal growth factor-like growth factor; MEK, mitogen-activated protein kinase/extracellular signal-regulated kinase; 3T3-L1/HB-EGF-AP, 3T3-L1 with stable expression of AP-tagged proHB-EGF.

kinase/extracellular signal-regulated kinase pathway (18). The insulin-induced HB-EGF shedding in 3T3-L1/HB-EGF-AP adipocytes was significantly suppressed by U0126 and PD98059 ($P < 0.01$) (**Figure 2a** and **Supplementary Figure S4a** online). Expression of HB-EGF mRNA was also significantly suppressed in 3T3-L1 adipocytes treated with U0126 and PD98059 relative to vehicle-treated groups ($P < 0.01$) (**Figure 2b**). On the other hand, insulin-induced HB-EGF shedding in 3T3-L1/HB-EGF-AP adipocytes was not suppressed and rather increased by a phosphoinositide 3-kinase inhibitor LY294002 ($P < 0.01$) (see **Supplementary Figure S4c** online).

Role of ADAM17 in insulin-induced HB-EGF shedding in 3T3-L1 adipocytes

Because there are numerous proteolytic enzymes expressed in adipocytes *in vitro* or in the adipose tissue *in vivo* (7,8), it is important to know which MMPs and/or ADAMs are involved in insulin-induced HB-EGF shedding in adipocytes. Quantitative real-time PCR analysis revealed significant amount of mRNAs for MMP3 and ADAMs 9, 10, 12, and 17, which are known to cleave proHB-EGF in COS-7 cells, mouse embryonic fibroblasts, or tumor cells (10,19), in differentiated 3T3-L1 adipocytes (**Figure 3a**). Expression of mRNAs for MMP3 and ADAM17 were significantly increased in 3T3-L1 adipocytes treated with insulin at a dose of 100 nmol/l (MMP3: $P < 0.05$; ADAM17: $P < 0.01$).

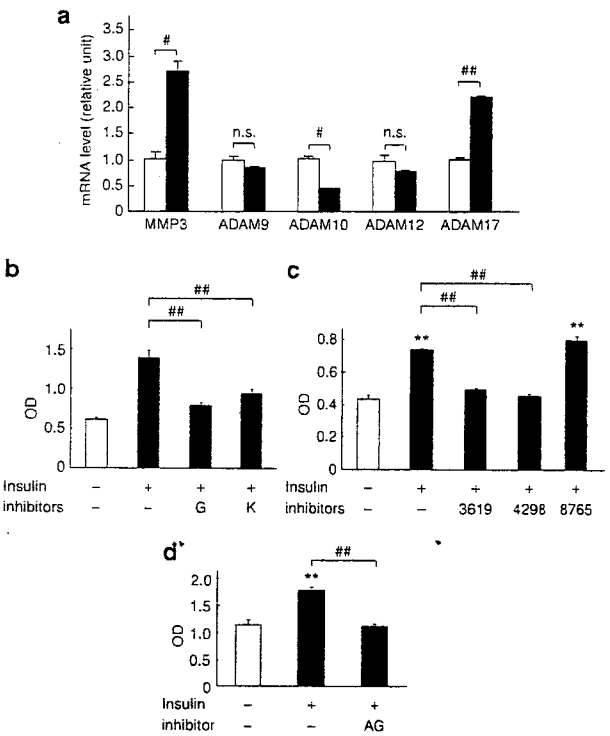

Figure 3 Effect of insulin on metalloprotease mRNA expression and effect of metalloprotease inhibitors and EGFR antagonist on insulin-induced HB-EGF shedding in 3T3-L1 adipocytes. (**a**) Expression of MMP and ADAM mRNAs in differentiated 3T3-L1 adipocytes treated with or without insulin for 24 h. Open bars, vehicle; filled bars, insulin (100 nmol/l). The results are expressed as mRNA levels relative to those in vehicle-treated groups, which were arbitrarily set at 1.0. (**b**) Effect of broad metalloprotease inhibitors on HB-EGF shedding in differentiated 3T3-L1/HB-EGF-AP adipocytes treated with insulin for 48 h. Optical density (OD) shows the absorbance at 405 nm, which indicates AP activity in the conditioned media. Open bar, vehicle; filled bars, insulin (100 nmol/l) with or without inhibitors. G, GM6001 (20 μmol/l); K, KB-R7785 (10 μmol/l). (**c**) Effect of ADAM-selective inhibitors on HB-EGF shedding in 3T3-L1/HB-EGF-AP adipocytes treated with insulin for 48 h. Open bar, vehicle; filled bars, insulin (100 nmol/l) with or without inhibitors. 3619, INCB3619 (1 μmol/l); 4298, INCB4298 (1 μmol/l); 8765, INCB 8765 (1 μmol/l). (**d**) Effect of EGFR antagonist on insulin shedding in differentiated 3T3-L1/HB-EGF-AP adipocytes treated with insulin for 48 h. Open bar, vehicle; filled bars, insulin (100 nmol/l) added with or without AG1478. AG, AG1478 (20 μmol/l). $^{**}P < 0.01$ vs. vehicle. $^{\#}P < 0.05$. $^{\#\#}P < 0.01$. $n = 4$–6. ADAM, a disintegrin and metalloproteinase; AP, alkaline phosphatase; EGFR, epidermal growth factor receptor; HB-EGF, heparin-binding EGF-like growth factor; MMP, matrix metalloproteinase; n.s., not significant; 3T3-L1/HB-EGF-AP, 3T3-L1 with stable expression of AP-tagged proHB-EGF.

The insulin-induced HB-EGF shedding in 3T3-L1/HB-EGF-AP adipocytes was significantly suppressed by broad metalloprotease inhibitors (**Table 2**) (20–24), GM6001 ($P < 0.01$ for insulin 100 nmol/l; $P < 0.05$ for insulin 10 nmol/l) and KB-R7785 ($P < 0.01$) (**Figure 3b** and **Supplementary Figure S4b** online). Importantly, there was a significant reduction in insulin-induced HB-EGF shedding in 3T3-L1/HB-EGF-AP adipocytes treated with INCB3619 and INCB4298, ADAM10/17-selective and ADAM17-selective inhibitors,